Designing Atomically Precise and Robust Covalent Organic Frameworks for Enhanced Iodine/Iodate Uptake：Structures with and without Phenol Hydroxy Groups

Qianyi Zuo,[1] *Xin Zheng,*[1,2] *Aokun Jia,*[1] *Tao Jiang, Bing Han,*[1,*] *Jiahong Pan,*[2] *Zhuoyu Ji,*[1,*]

[1] MOE Key Laboratory of Resources and Environmental Systems Optimization, College of Environmental Science and Engineering, North China Electric Power University, Beijing 102206, China

[2] State Key Laboratory of Featured Metal Materials and Life-Cycle Safety for Composite Structures, School of Resources, Environments and Materials, Guangxi University, Nanning 530004, China

* Corresponding authors.

E-mail: jizhuoyu@ncepu.edu.cn (Zhuoyu Ji); hanbing01@ncepu.edu.cn (Bing Han).

1. Materials and Characterization

Tri(4-aminophenyl)amine (TAPA, 98%), 2,5-dihydroxyterephthalaldehyde (Dha, 97%) were procured from Shanghai Haohong Biomedical Technology Co., Ltd. (China). 1,3,5-Benzenetricarboxaldehyde (BT, 97%), p-phthalaldehyde (PDA, 98%) were purchased from Shanghai Bide Pharmaceutical Technology Co., Ltd. (China). All solvents were purchased in analytical purity from Energy-Chemical, or Macklin Biochemical Co., Ltd. (Shanghai). All chemicals were used as received without any further purification.

Fourier-transformed infrared spectroscopy (FT-IR) were acquired on a SHIMADZU IRTracer-100 spectrometer in the range of 4,000 to 400 cm^{-1}. The powder X-ray diffraction (PXRD) patterns were collected using a Rigaku SmartLab SE diffractometer from 2.5° to 40°. The morphology and element mapping were recorded using scanning electron microscope combined with an energy dispersive spectrometer (SEM-EDS, EVO18) at an accelerating voltage of 10 kV. UV-vis absorption studies were performed on a Shimadzu UV 2700 UV/vis spectrophotometer in an optical quartz cuvette (10 mm path length) over the entire range of 600-250 nm. The XPS spectra were obtained with a Thermo Scientific Nexsa G2, and the surface charging effect was calibrated using the C 1s peak at 284.8 eV. The zeta potential was detected by Zetasizer Nano ZSE. The Raman spectra were obtained using a HORIBA Instroments Incorporated iHR550 Raman spectrometer with a 532 nm laser.

2. Synthesis

2.1 Preparation of COF-BT

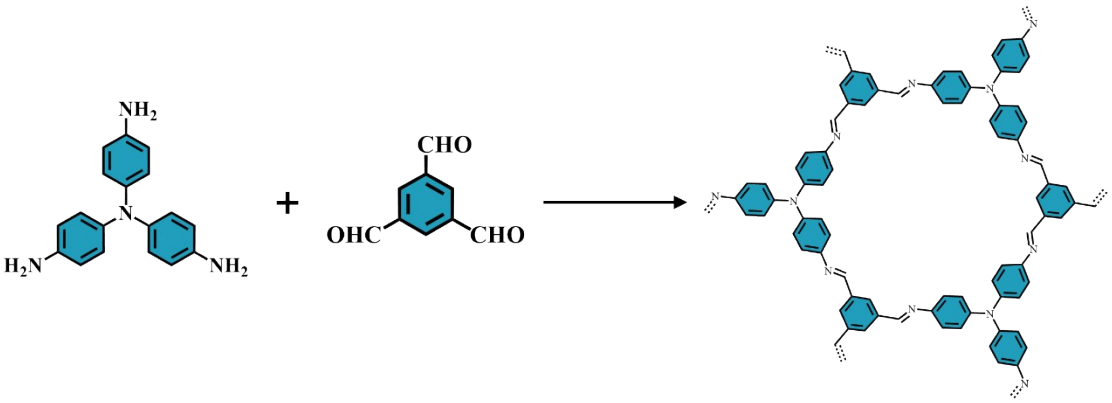

COF-BT was synthesized by using a solvothermal method. Initially, TAPA (50.22 mg, 0.4 mmol) and BT (67.01 mg, 0.4 mmol) were added in a 10 mL round-bottomed flask with 2 mL of a 1,2-dichlorobenzene/1-butanol solution (1:1 v/v), then 0.2 mL of acetic acid (6 M) was added. Subsequently, after sonicated for 5 min to be dispersed homogeneously, the tube was flash-frozen at 77 K using a liquid N_2 bath and degassed by three freeze-pump-thaw cycles, sealed under vacuum, and last heated at 120 °C for 3 days. The precipitate was collected by centrifugation and washed with DMF and THF. The collected sample was solvent-exchanged with acetone 2-3 times and dried at 120 °C under vacuum for 12 h. The resulting yellow powder was designated as COF-BT.

2.2 Preparation of COF-TP

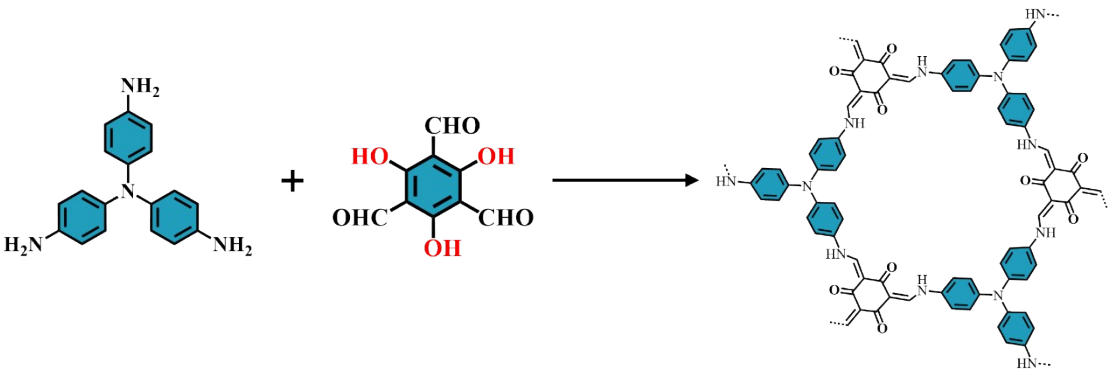

COF-TP was synthesized by using a solvothermal method as Ahmed *et.al*..[1] Firstly,

TAPA (50.22 mg, 0.4 mmol) and TP (67.01 mg, 0.4 mmol) were added in a 10 mL round-bottomed flask with 5 mL of a 1,2-dichlorobenzene/1-butanol solution (1:1 v/v), then 0.5 mL of acetic acid (6 M) was added. After sonicated for 5 min to be dispersed homogeneously, the tube was flash-frozen at 77 K using a liquid N_2 bath and degassed by three freeze-pump-thaw cycles, sealed under vacuum, and last heated at 120 °C for 3 days. The precipitate was collected by centrifugation and washed with DMF and THF. The collected sample was solvent-exchanged with acetone 2-3 times and dried at 120 °C under vacuum for 12 h. The resulting red-brown powder was designated as COF-BT.

2.3 Preparation of COF-Dha

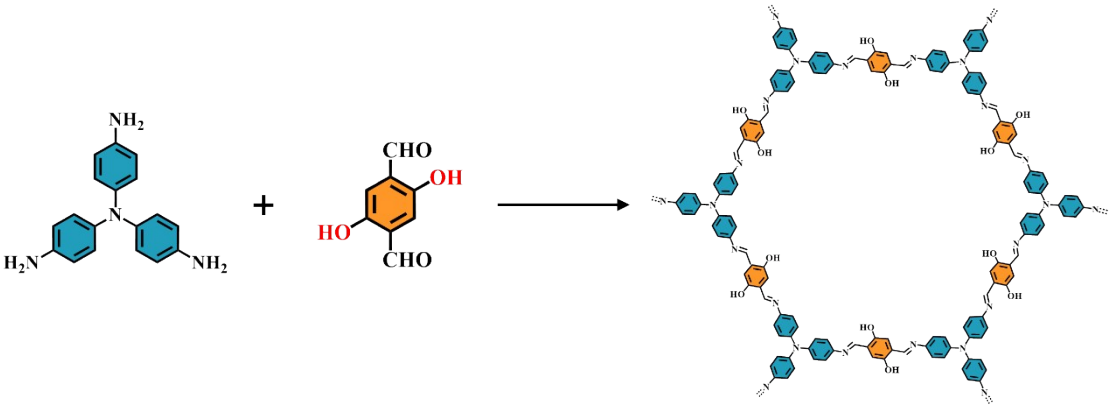

The preparation of COF-Dha is the same as Huang *et al*..[2] A 10 mL Pyrex tube was charged with TAPA (6 mg, 0.02 mmol), Dha (5 mg, 0.03 mmol) and anisole/1-butanol (9:1 v/v, 1 mL). The mixture was sonicated for 5 min to be dispersed homogeneously. Next, 0.2 mL of acetic acid (6 M) was added. Subsequently, the tube was flash-frozen at 77 K using a liquid N_2 bath and degassed by three freeze-pump-thaw cycles, sealed under vacuum, and then heated at 120 °C for 3 days. The precipitate was collected by centrifugation and washed with tetrahydrofuran. The collected sample was solvent-

exchanged with acetone 2-3 times and dried at 120 °C under vacuum for 12 h, and finally red powder was obtained.

2.4 Preparation of COF-PDA

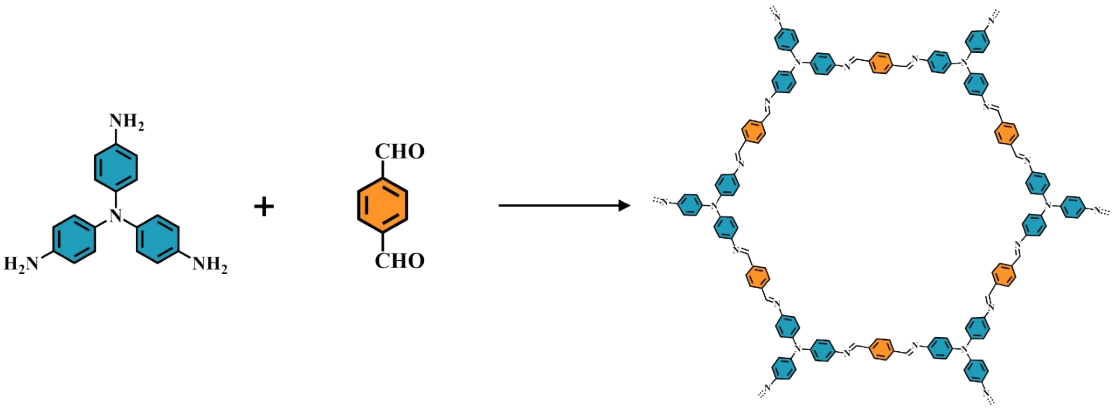

COF-PDA was synthesized by following a previously reported procedure.[3] TAPA (46.5 mg, 0.16 mmol) and PDA (32.16 mg, 0.24 mmol) were combined in a 10 mL Pyrex tube with a 1,2-dichlorobenzene/1-butanol solution (1:1 v/v, 2 mL), and the resulting suspension was sonicated at room temperature until the monomers were fully dissolved. Next, 0.2 mL of acetic acid (6 M) was added and sonicated for 5 min to be dispersed homogeneously. Subsequently, the tube was flash-frozen at 77 K using a liquid N_2 bath and degassed by three freeze-pump-thaw cycles, sealed under vacuum, and then heated at 120 °C for 3 days. The precipitate was collected by centrifugation and washed with DMF. The collected sample was solvent-exchanged with acetone 2-3 times and dried at 120 °C under vacuum for 12 h, and finally red powder was obtained.

3 Experimental sections

3.1 Gas-phase iodine adsorption experiment

Typically, ~15 mg of COFs sample were weighted in a small glass vial, and this vial was exposed to I_2 (20 mg) or CH_3I (~3 mL) at 75 °C (348 K) in a closed system respectively. After the corresponding adsorption time, the glass vial was taken out, cooled to room temperature and weighed. The uptake capacity of the sample was calculated by the weight difference of glass vials before and after adsorption, using the equation (1).

$$W = \frac{m_2 - m_1}{m_1} \times 100\% \quad (1)$$

Where, W (g g^{-1}) is the adsorption capacity of organic polyiodide uptake, m_1 (g) and m_2 (g) are the mass of COFs before and after being exposed to I_2 or CH_3I vapor. The values of uptake capacity are the average values of at least three experiments.

3.2 I_2 (cyclohexane) adsorption experiment

Adsorption kinetics study: Preparing a 5 mL iodine-cyclohexane of I_2 (100 ppm,) in a 5 mL glass bottle, followed by the addition of 5 mg adsorbent (dosage = 1 g/L), and stirred at room temperature for 24 h to ensure equilibrium adsorption. The change of the absorbance of supernatant at 523 nm was recorded by UV-vis spectroscopy at a certain time interval. The kinetics data of I_2 (cyclohexane) adsorption were fitted by pseudo-first order model expressed as equation (2) and pseudo-second order model expressed as equation (3).

$$\ln\left(q_e - q_t\right) = lnq_e - k_1 t \quad (2)$$

$$\frac{t}{q_e} = \frac{1}{k_2 q_e^2} + \frac{t}{q_e} \quad (3)$$

Where k_1 (min^{-1}) and k_2 (g g^{-1} min^{-1}) stand for the corresponding rate constants, q_e and q_t (g/g) are the adsorption capacity at equilibrium and time t (min), respectively.

For adsorption isotherms study, 5 mg adsorbent was added into 5 mL I_2-cyclohexane solutions with a series of concentration gradients of 200 ppm to 1600 ppm, stirred at room temperature for 48 h until adsorption equilibrium, then filtered by 0.22 μm membrane filter, and recorded the absorbance value of I_2 with UV-vis spectroscopy. The Langmuir adsorption isotherm (4) and Freundlich adsorption isotherm (5) were used for fitting.

$$\frac{C_e}{q_e} = \frac{1}{q_m K_L} + \frac{C_e}{q_m} \quad (4)$$

$$lnq_e = \ln K_F + \frac{1}{n} lnC_e \quad (5)$$

Where C_e (mg/L) is the equilibrium concentration of I_2 (cyclohexane), q_m (g/g) is the maximum adsorption capacity, K_L and K_F are the Langmuir constant and the Freundlich constant, respectively. n is a constant related to sorption intensity.

3.3 I_2 (aqueous) adsorption experiment

To investigate the kinetics of I_2 (aqueous) adsorption by the adsorbent, several sealed vials were prepared, each containing 5 mL of 100 mg/L iodine solution and 0.5 mg of adsorbent (dosage = 0.1 g/L). The vials were stirred at room temperature for 24 h to ensure equilibrium adsorption, and samples were taken at different time intervals using a saturated filter head. The iodine adsorption amount was measured using a UV-Vis spectrophotometer from 600-250 nm.

3.4 Polyiodide adsorption experiment

Adsorption kinetics study: Preparing a 5 mL aqueous solution of polyiodide (50 ppm, [KI]/[I_2] = 2/1) in a 5 mL glass bottle, followed by the addition of 0.5 mg adsorbent (dosage = 0.1 g/L), and stirred at room temperature for 24 h to ensure equilibrium adsorption. The change of the absorbance of supernatant at 355 nm was recorded by UV-vis spectroscopy at a certain time interval, and the adsorption kinetics were calculated and fitted.

For adsorption isotherms study, 0.5 mg adsorbent was added into 5 mL polyiodide aqueous solutions with a series of concentration gradients of 70 ppm to 250 ppm, stirred at room temperature until adsorption equilibrium, then filtered by 0.22 μm membrane filter, and recorded the absorbance value of polyiodide with UV-vis spectroscopy.

For competitive sub-adsorption experiment, 1 mg adsorbent was added into 5 mL 5 mM polyiodide and 50 mM different anions aqueous solutions, stirred at room temperature 24 h until adsorption equilibrium, then filtered by 0.22 μm membrane filter, and recorded the absorbance value of polyiodide with UV-vis spectroscopy.

3.5 IO_3^- adsorption experiment

In order to solve the problem that IO_3^- has no characteristic peak in the UV spectrum, we measured the concentration of IO_3^- by introducing KI to convert IO_3^- into polyiodide under acidic conditions (Formulas 6-7). And the adsorption kinetics experiment and adsorption isotherm experiment are similar to I_2-cyclohexane adsorption experiment. For adsorption kinetics experiment, the initial concentration of IO_3^- is 50 mg L^{-1}, and the solid-liquid ratio of the adsorbent is 1 g/L. For adsorption isotherm experiment, a

2000 mg·L^{-1} IO_3^- stock solution was prepared and diluted to concentrations ranging from 50 to 600 mg·L^{-1}. In this case, 5 mL of the diluted IO_3^- solution was mixed with 5 mg of adsorbent and shaken for 48 h in dark to ensure equilibrium adsorption. The iodine adsorption was then measured at 355 nm, and the corresponding IO_3^- adsorption isotherm was fitted.

$$IO_3^- + 6H^+ + 5I^- = I_2 + H_2O \quad (6)$$

$$I_2 + I^- = I_3^- \quad (7)$$

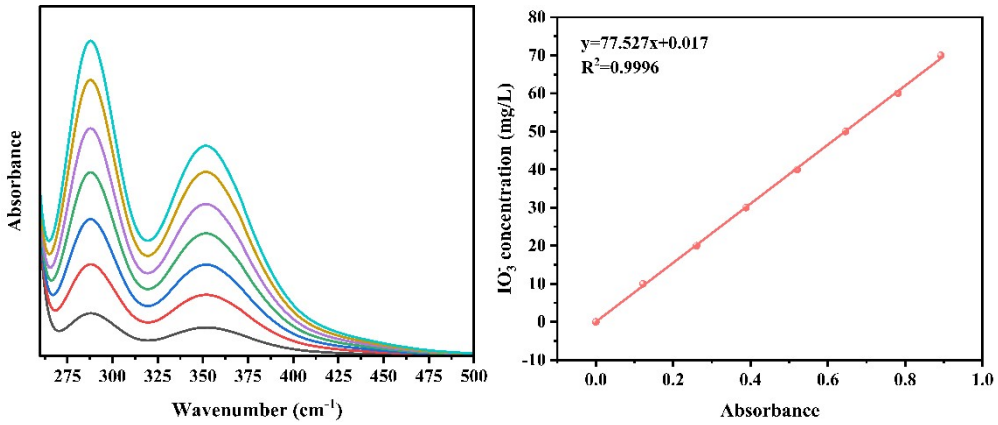

3.6 The recyclability test

For the recyclability experiment, 20 mg COF-Dha was adsorbed five times in 300 ppm iodate aqueous solution (solid-liquid ratio 1 g/L), 300 ppm I_2 aqueous solution (solid-liquid ratio 0.2 g/L) and 300 ppm polyiodide aqueous solution (solid-liquid ratio 0.2 g/L), respectively.

For the recovery of COF-Dha, the adsorbed COF-Dha was reduced to hydroquinone by ascorbic acid solution, and then treated with ethanol, saturated NaCl aqueous solution and 1M hydrochloric acid in turn. Finally, COF-Dha-R was obtained.

4.Supplementary Figures

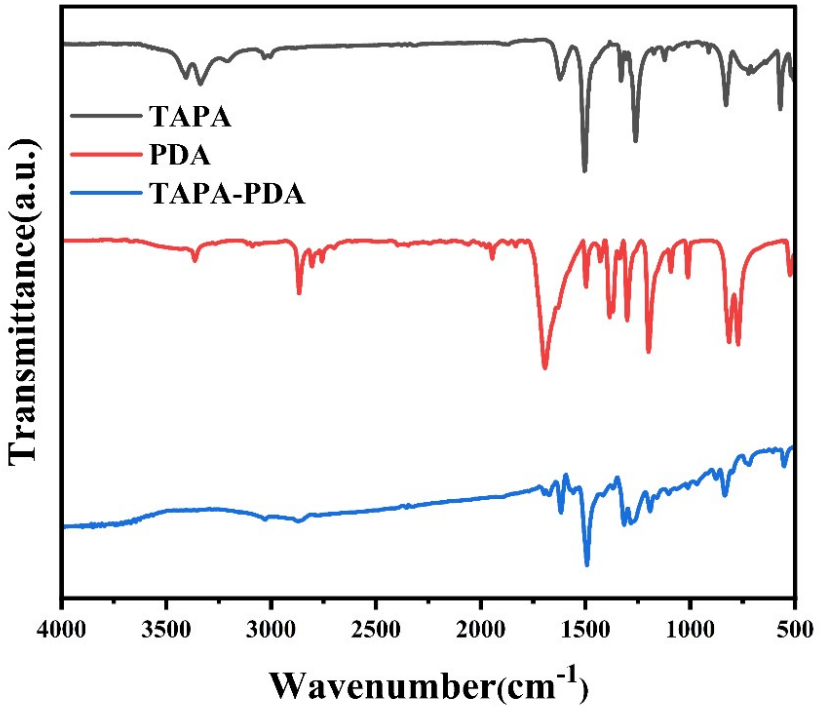

Figure S1. FT-IR spectra of TAPA-PDA and precursors.

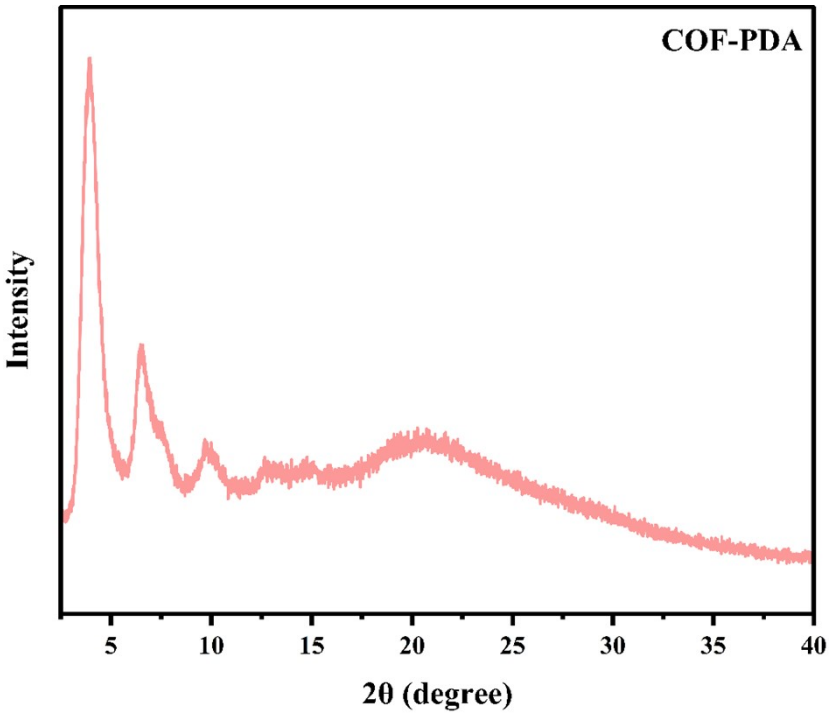

Figure S2. XRD spectra of COF-PDA.

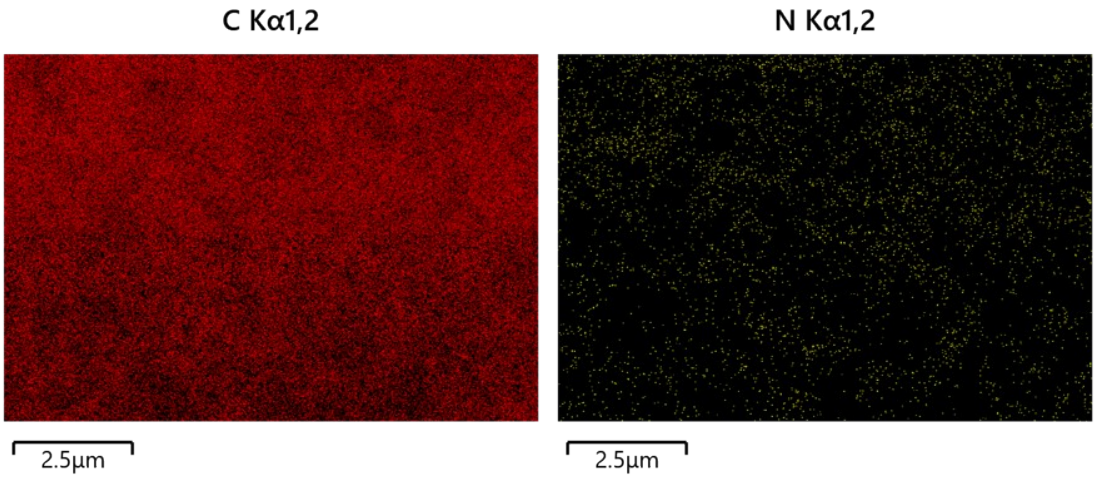

Figure S3. EDS mapping of COF-BT.

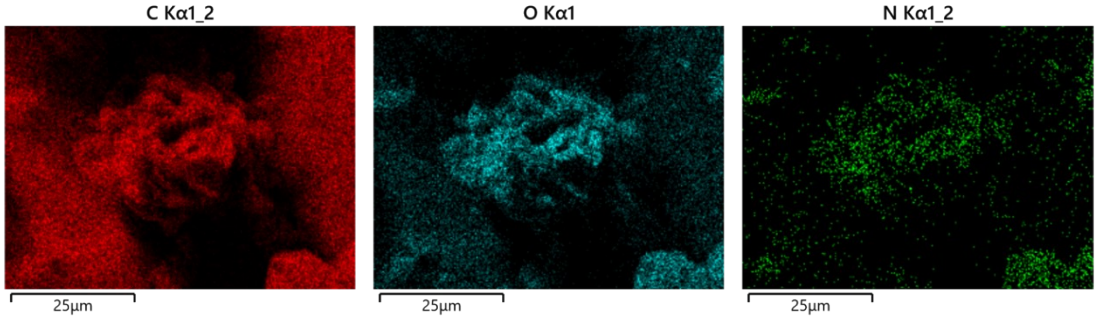

Figure S4. EDS mapping of COF-TP.

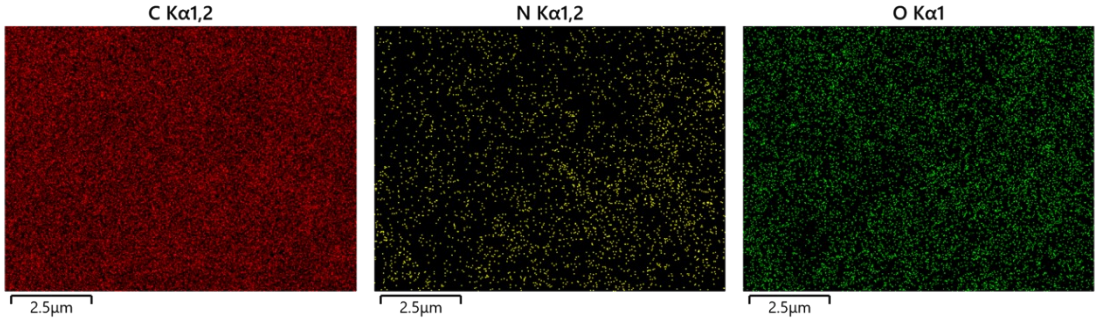

Figure S5. EDS mapping of COF-Dha.

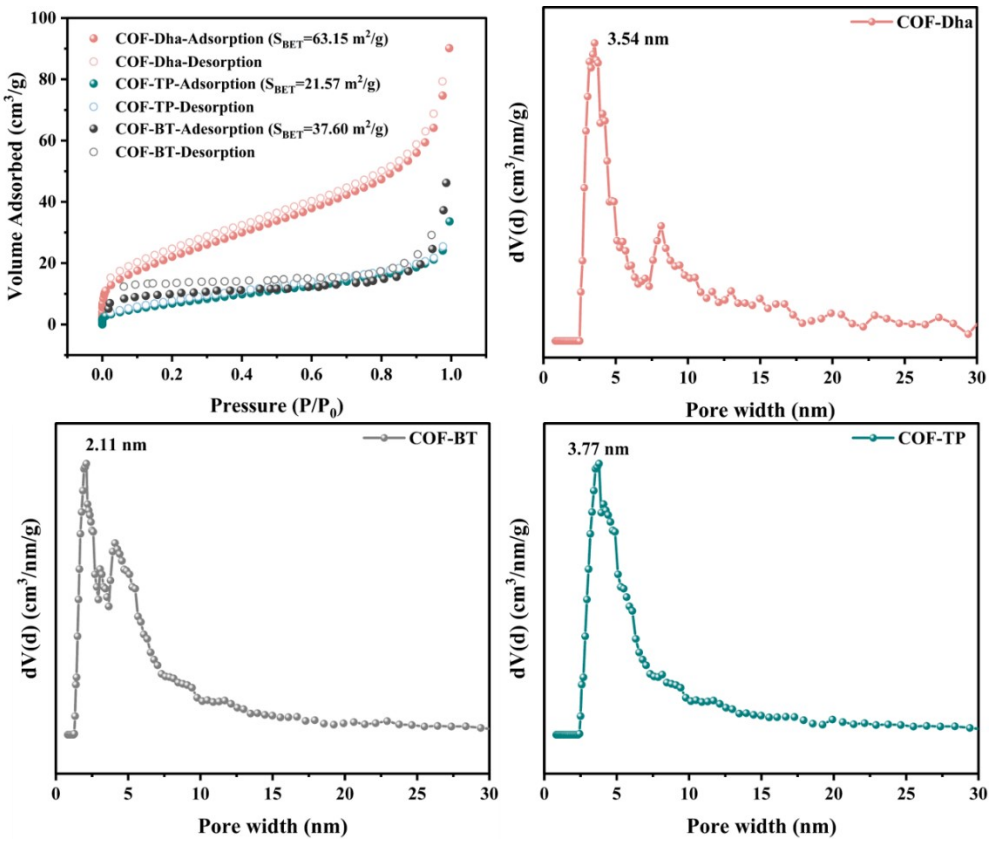

Figure S6. BET of COF-Dha, COF-BT and COF-TP

.

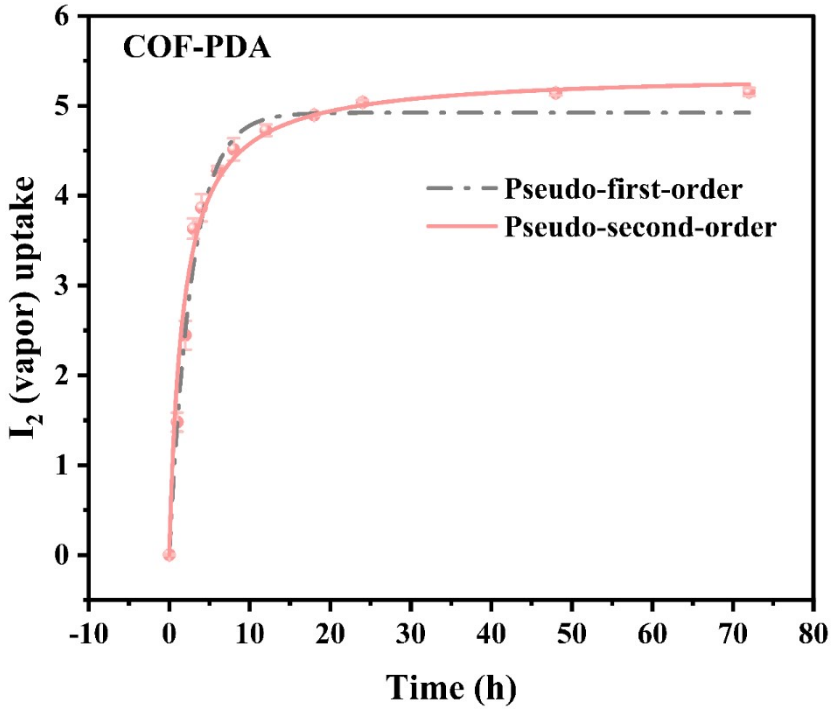

Figure S7. I_2 vapor adsorption curve of COF-PDA.

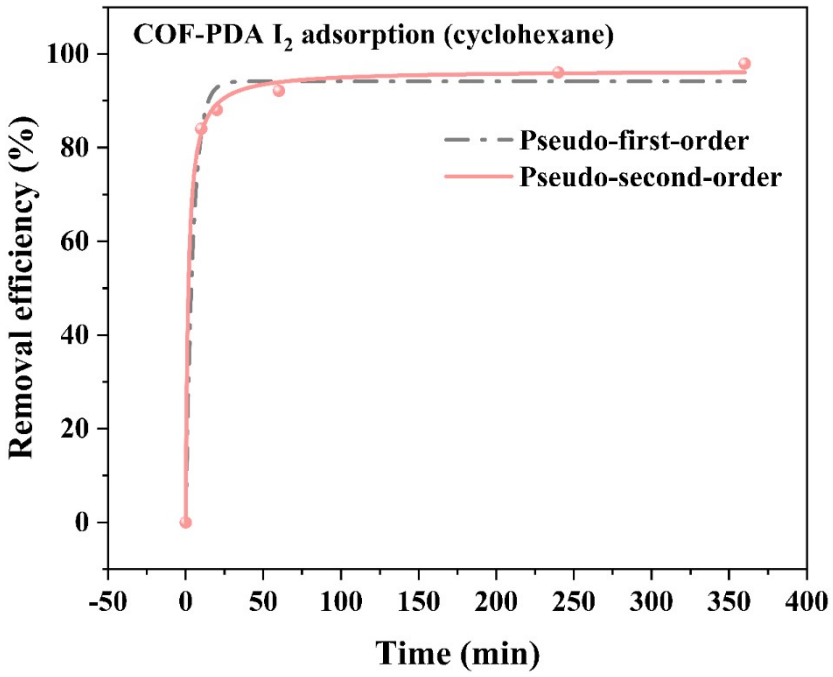

Figure S8. Adsorption kinetics of I_2 (cyclohexane) by COF-PDA.

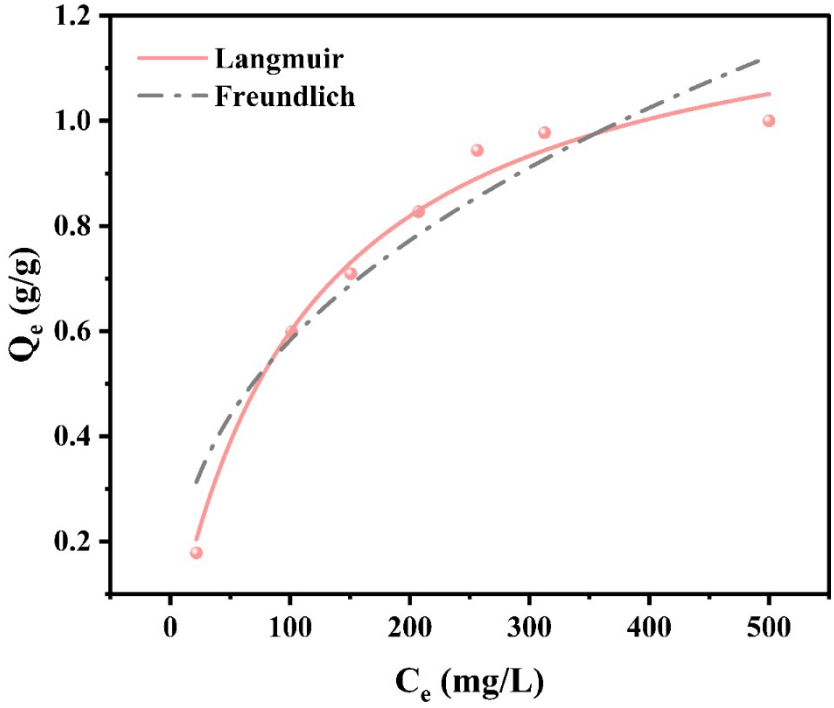

Figure S9. Adsorption isotherm for I_2 (cyclohexane) on COF-PDA.

Figure S10. Pictures of the process of COF-PDA adsorbing I_2 (aqueous). The color changed from yellow to transparent and final became blue, which indicate that COF-PDA experienced the process of adsorption and dissolution of iodine.

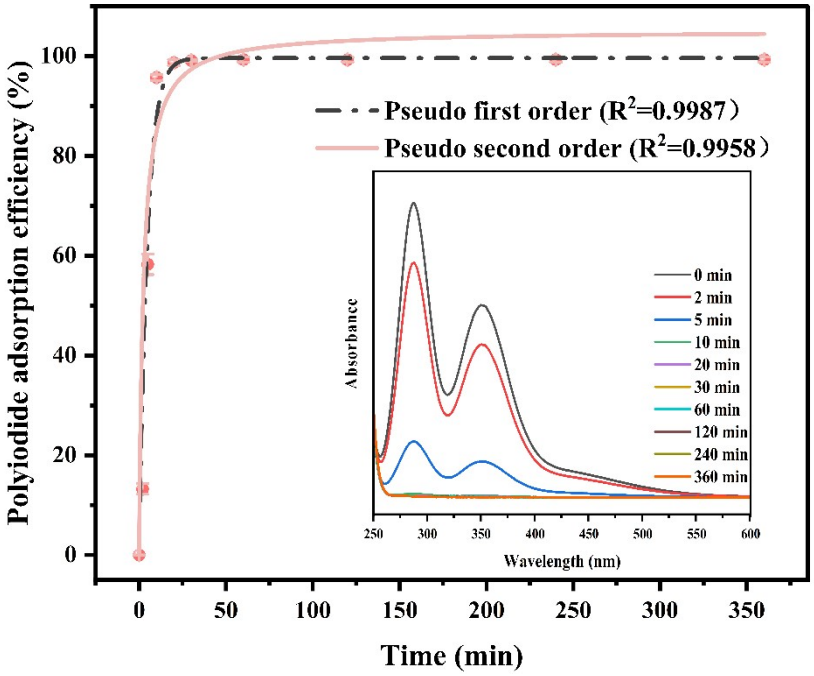

Figure S11. Adsorption kinetics of polyiodide (50 ppm) by COF-Dha.

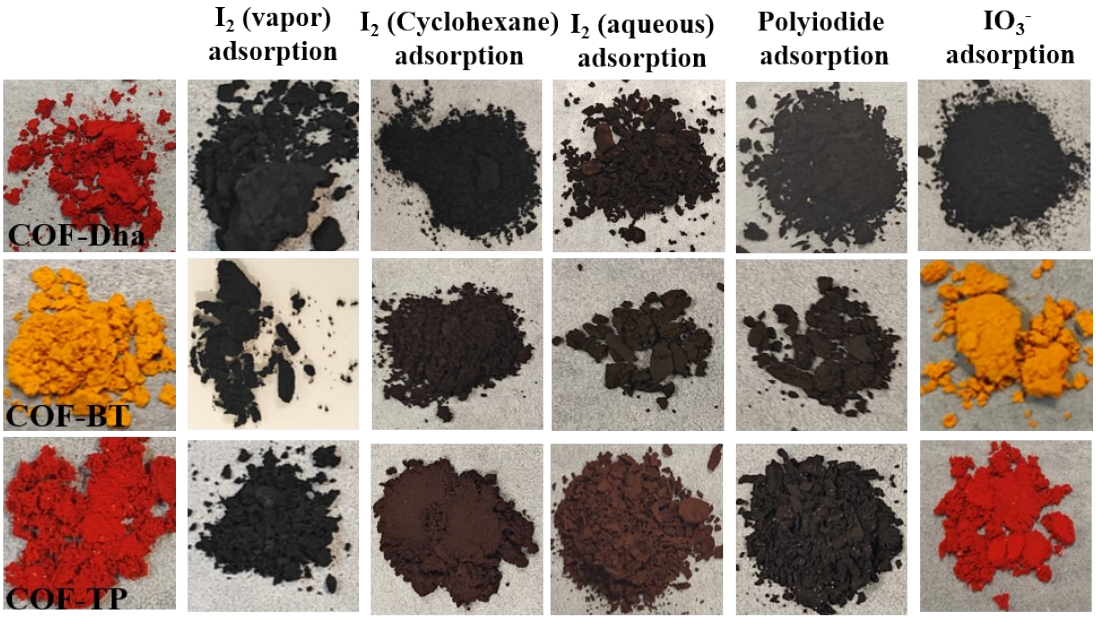

Figure S12. Pictures before and after different iodine species adsorption.

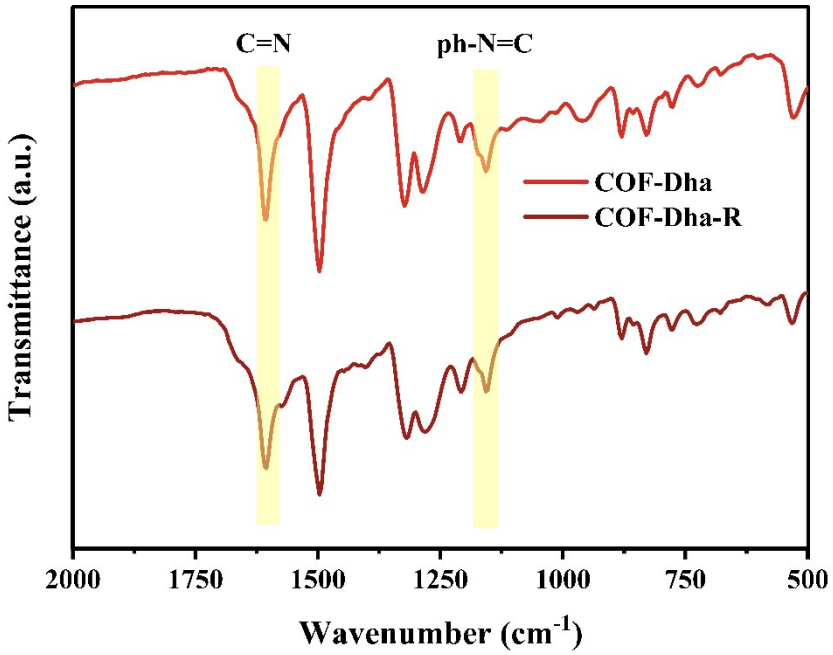

Figure S13. The FT-IR spectrum of COF-Dha and COF-Dha-R.

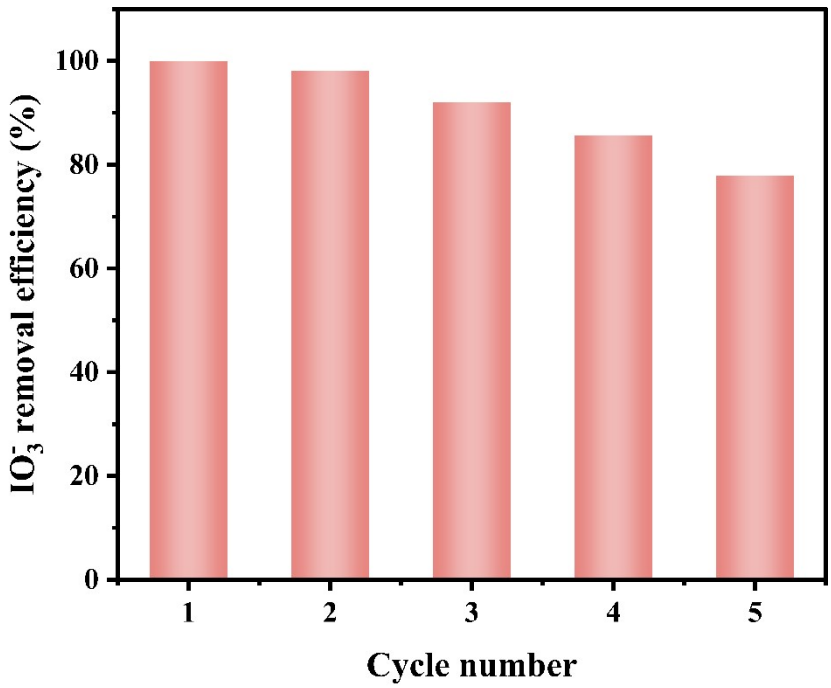

Figure S14. The recyclability experiment of COF-Dha on iodate.

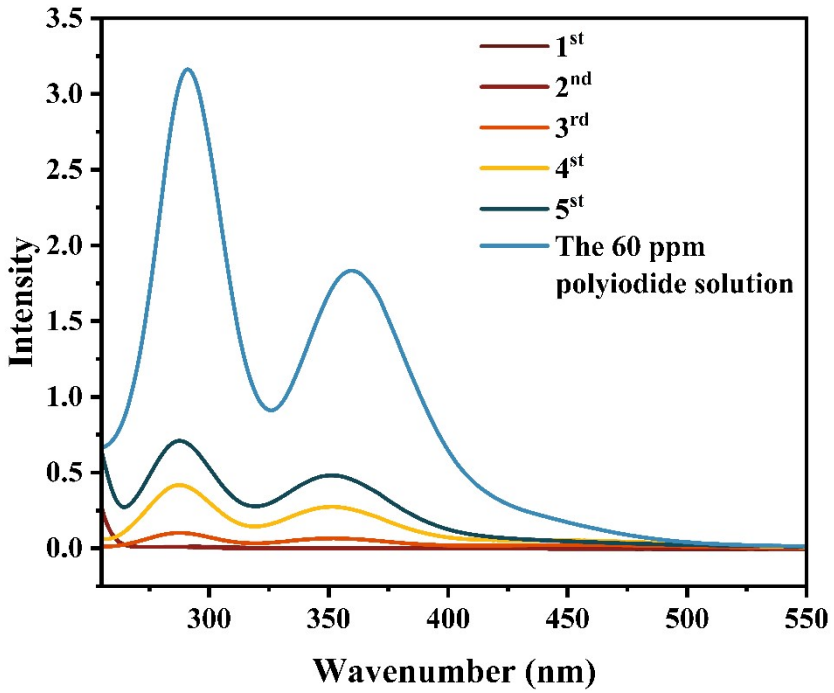

Figure S15. The UV/Vis spectrum of recyclability experiment of COF-Dha on I_2 aqueous.

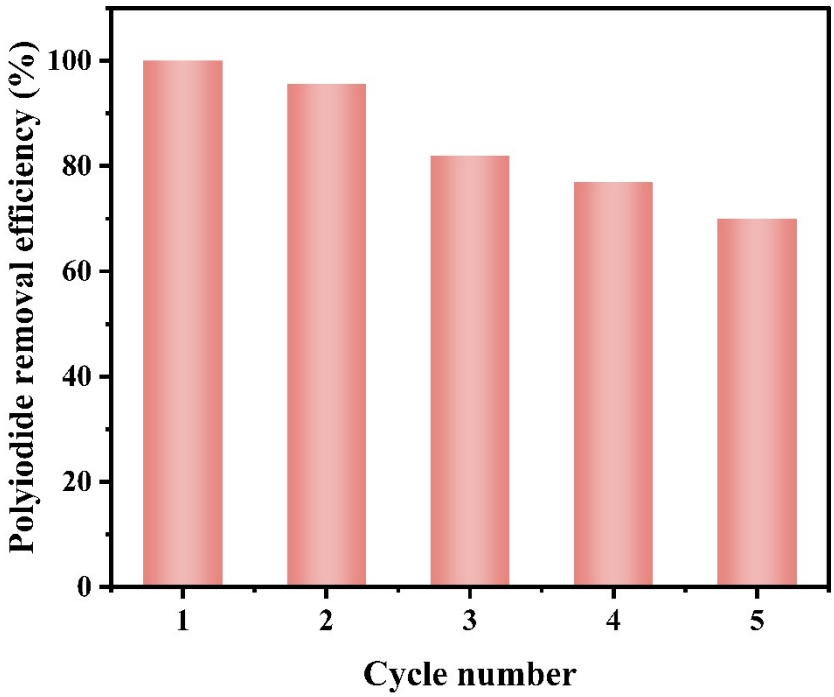

Figure S16. The recyclability experiment of COF-Dha on polyiodide solution.

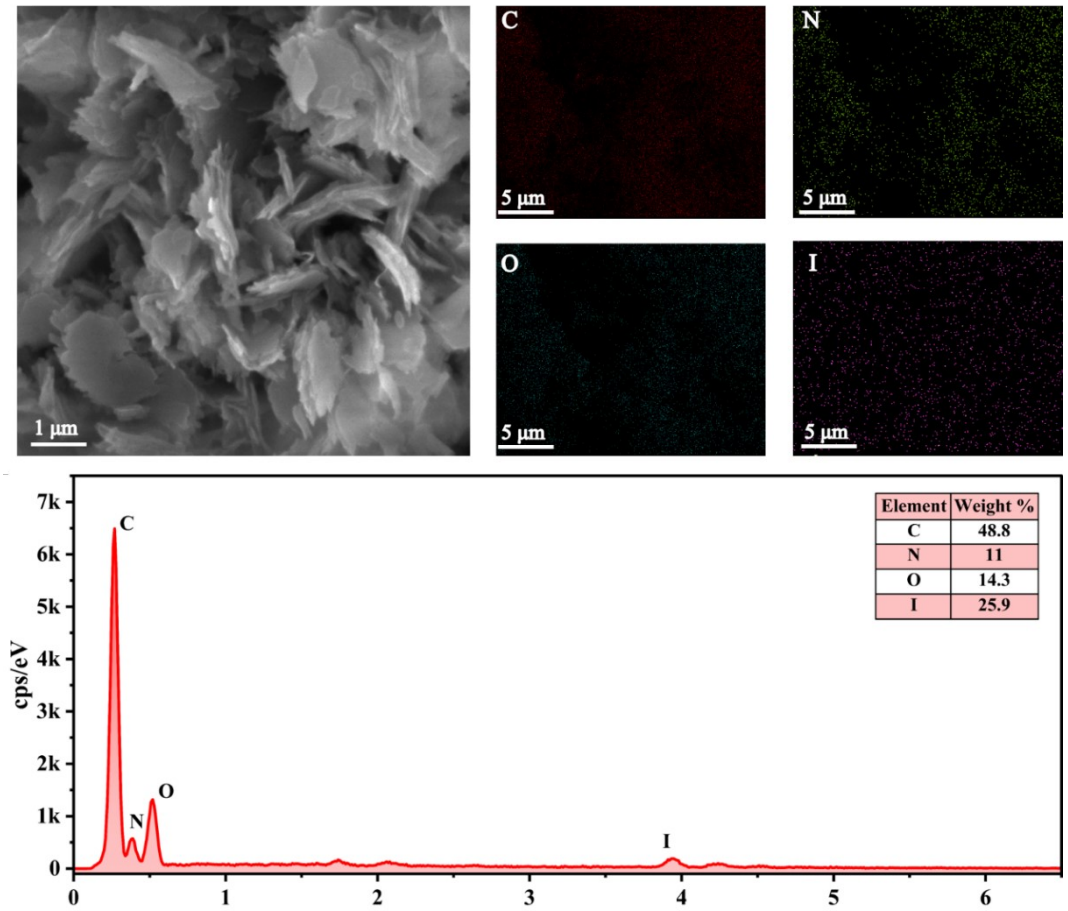

Figure S17. SEM image and EDS mapping of COF-Dha after I_2 (aqueous) adsorption.

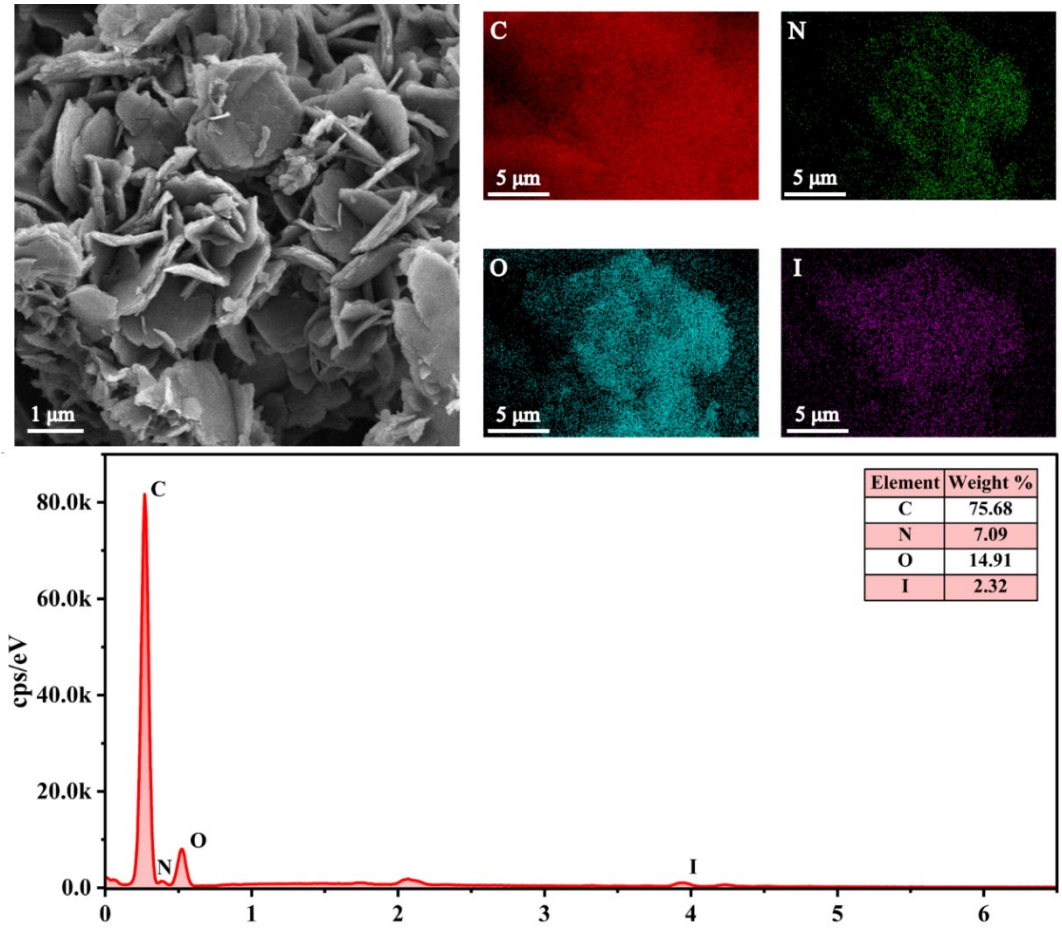

Figure S18. SEM image and EDS mapping of COF-Dha after IO_3^- adsorption.

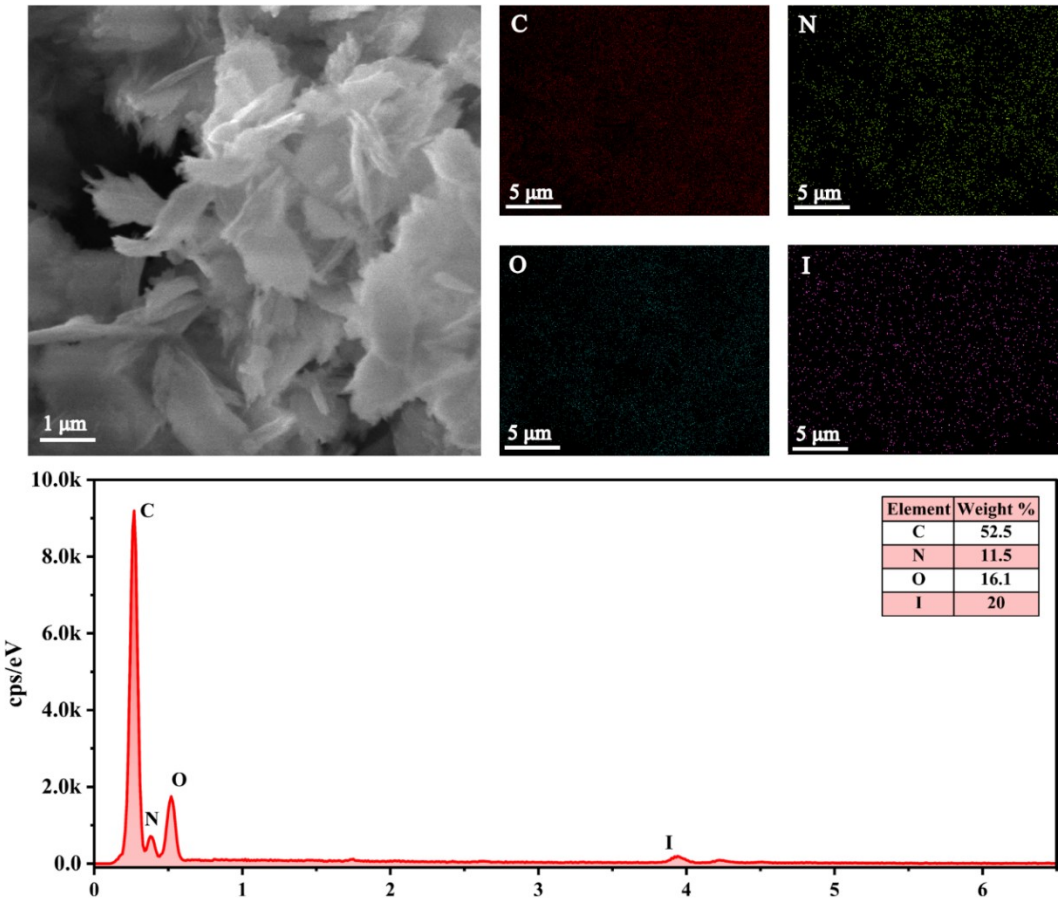

Figure S19. SEM image and EDS mapping of COF-Dha after polyiodide adsorption.

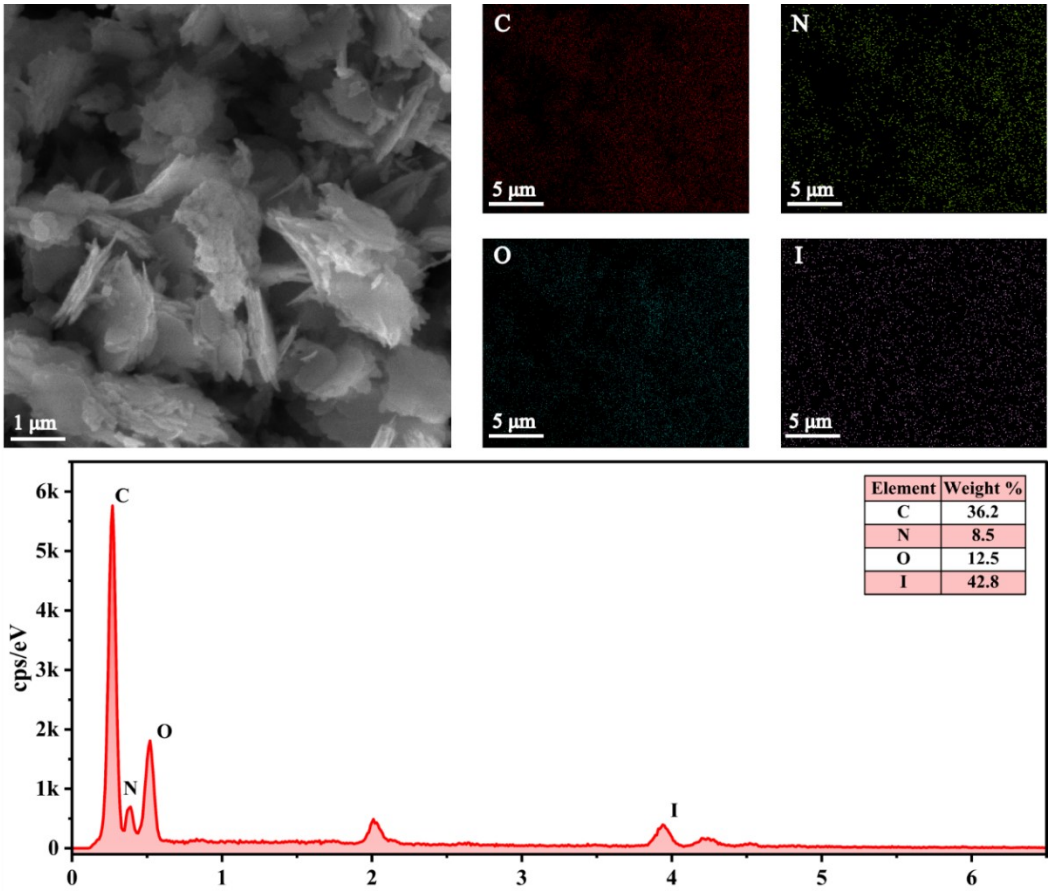

Figure S20. SEM image and EDS mapping of COF-Dha after I_2 (cyclohexane) adsorption.

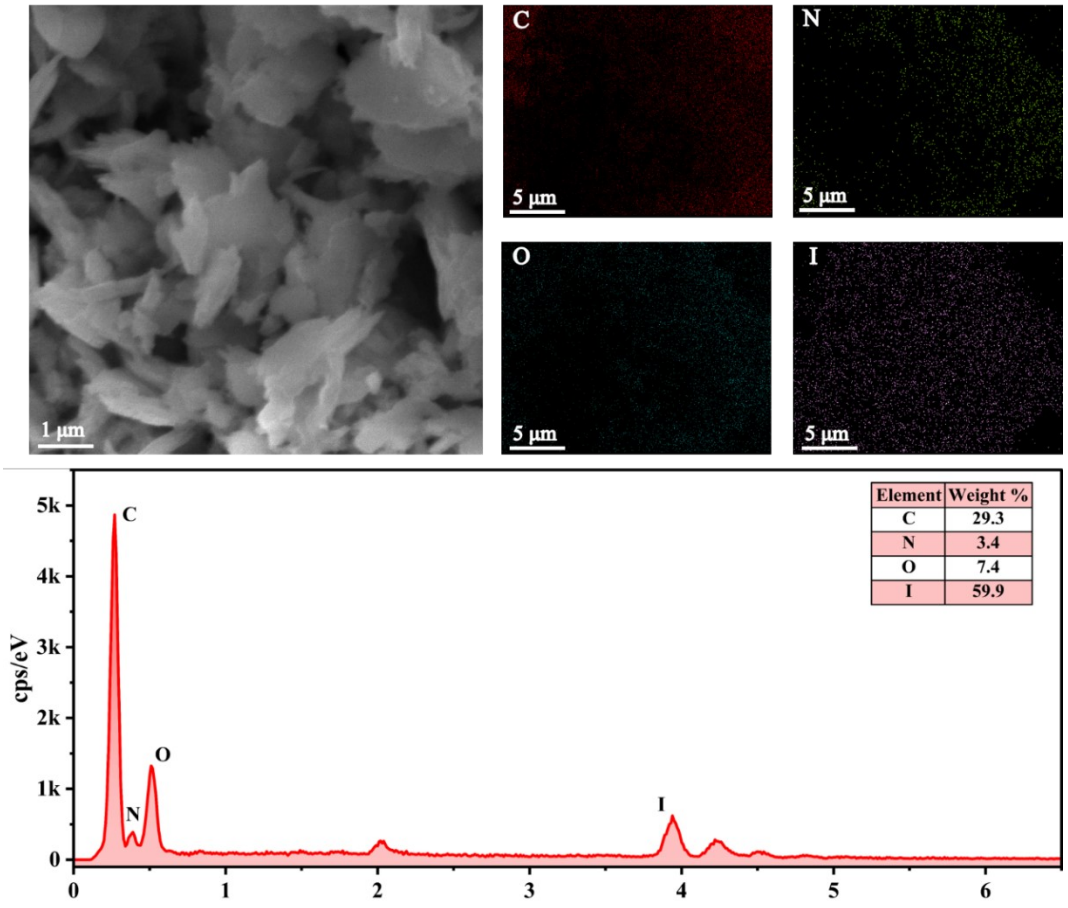

Figure S21. SEM image and EDS mapping of COF-Dha after I_2 (vapor) adsorption.

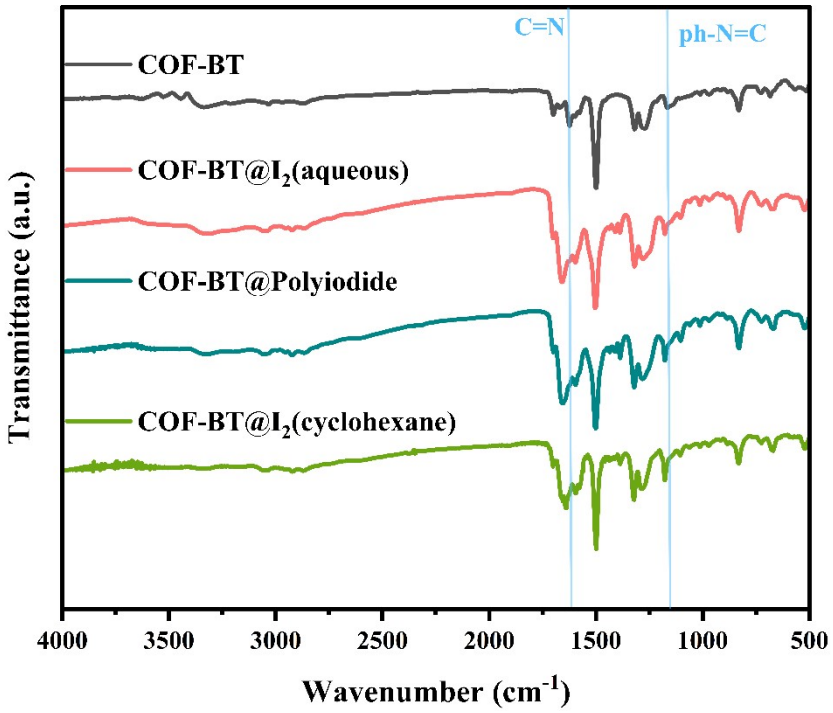

Figure S22. FT-IR spectra of COF-BT before (black) and after I_2 (aqueous) adsorption (pink), polyiodide adsorption (blue) and I_2 (cyclohexane) adsorption (green).

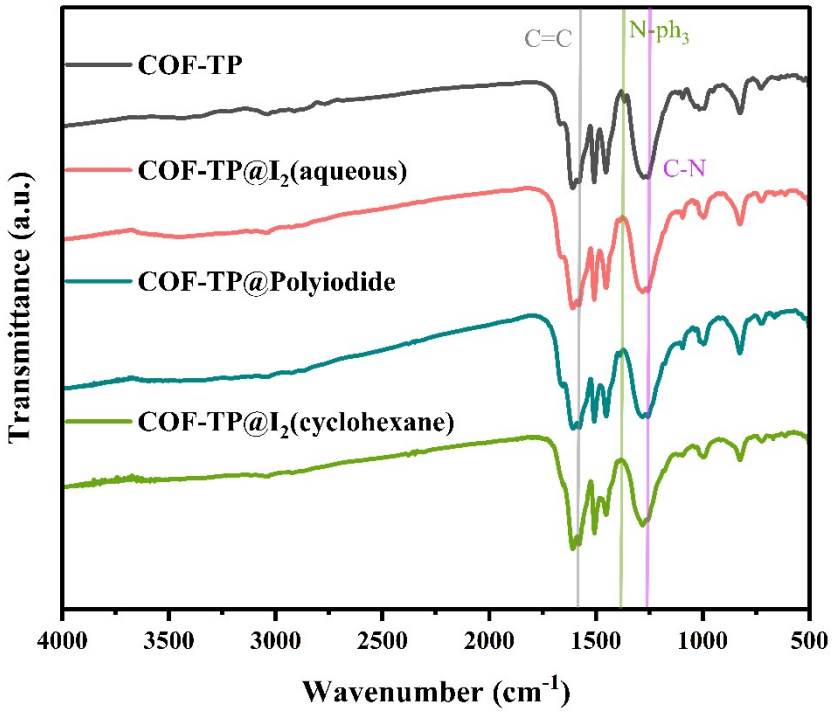

Figure S23. FT-IR spectra of COF-TP before (black) and after I_2 (aqueous) adsorption (pink), polyiodide adsorption (blue) and I_2 (cyclohexane) adsorption (green).

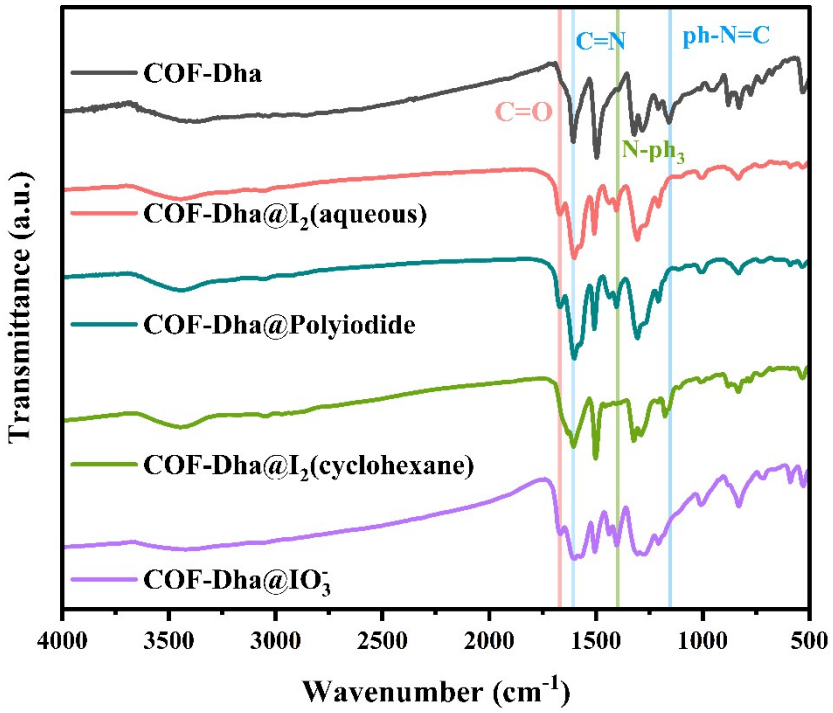

Figure S24. FT-IR spectra of COF-Dha before (black) and after I_2 (aqueous) adsorption (pink), polyiodide adsorption (blue), I_2 (cyclohexane) adsorption (green) and IO_3^- adsorption (purple).

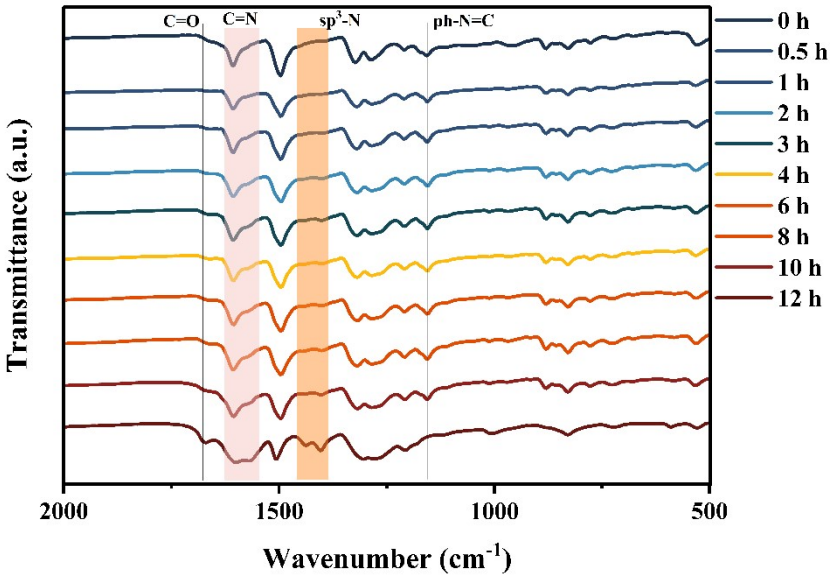

Figure S25. Time-dependent FT-IR spectra of COF-Dha during IO_3^- adsorption. (Initial concentration 300 ppm, solid-liquid ratio 1 g/L)

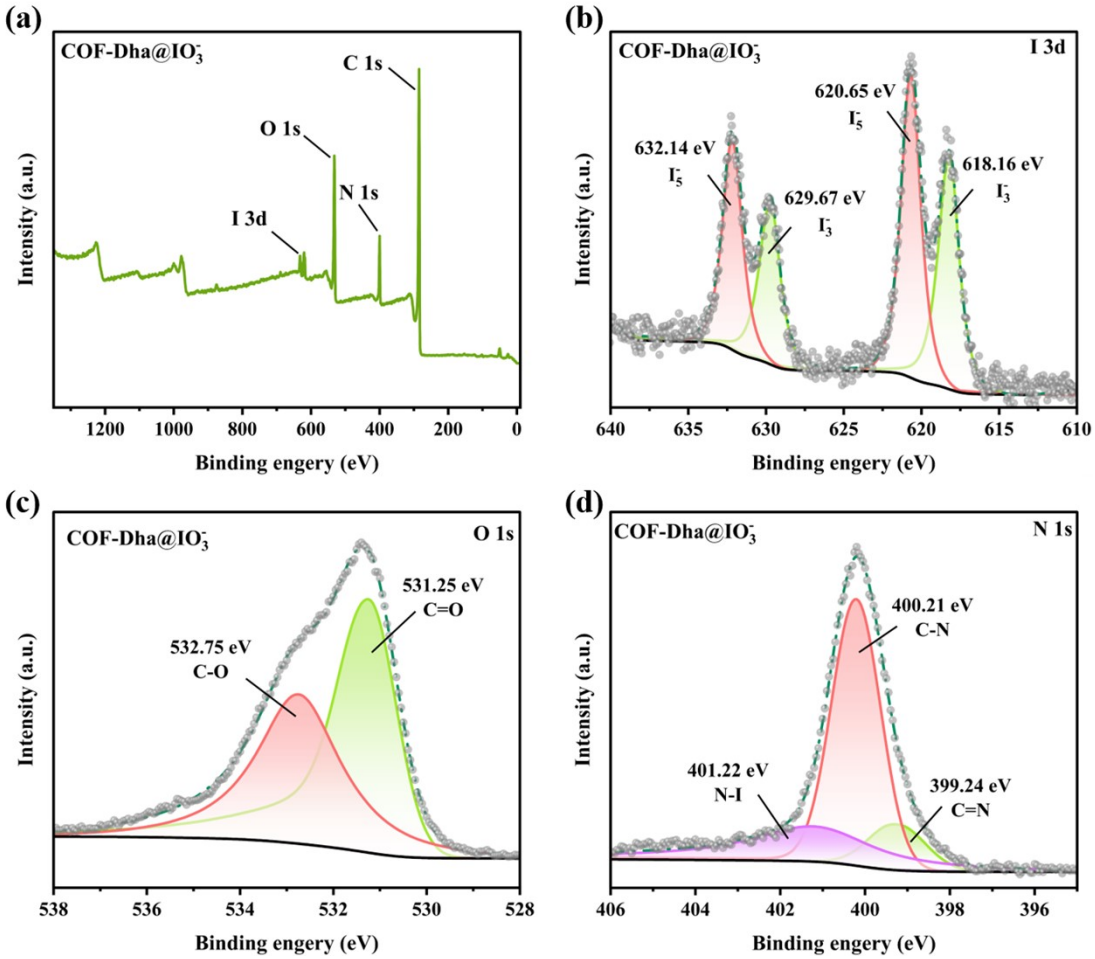

Figure S26. (a) Full survey XPS spectra of COF-Dha after IO_3^- adsorption. High-resolution XPS spectra of I 3d (b) O 1s (c) and N 1s (d) for COF-Dha after IO_3^- adsorption.

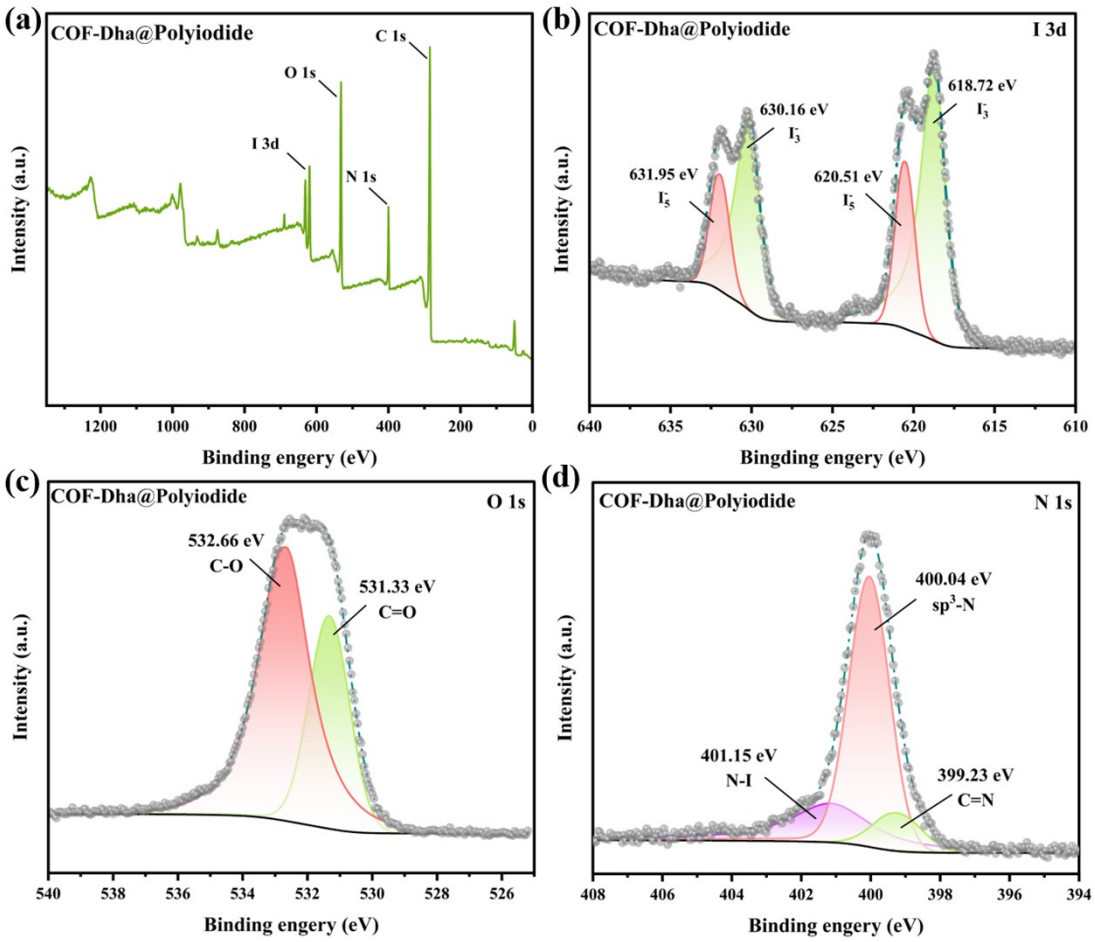

Figure S27. (a) Full survey XPS spectra of COF-Dha after polyiodide adsorption. High-resolution XPS spectra of I 3d (b) O 1s (c) and N 1s (d) for COF-Dha after polyiodide adsorption.

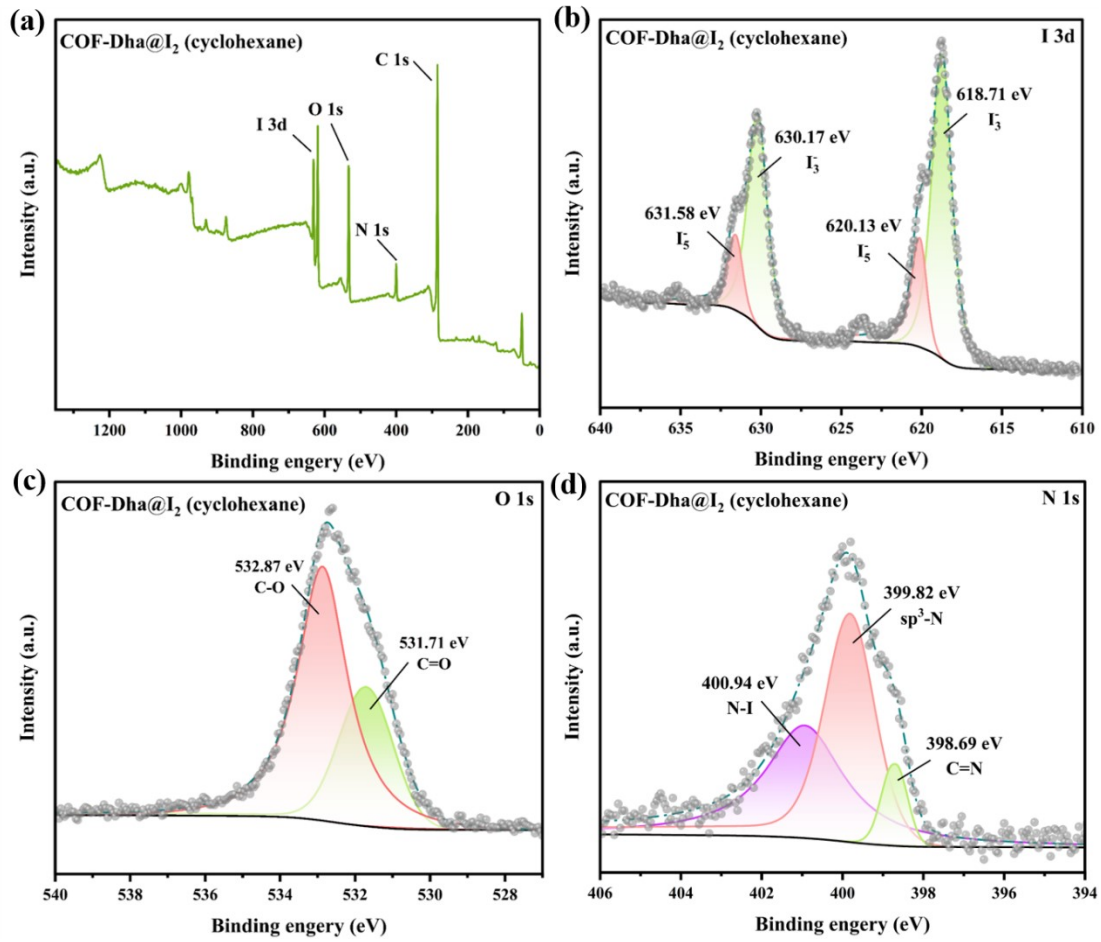

Figure S28. (a) Full survey XPS spectra of COF-Dha after I_2 (cyclohexane) adsorption. High-resolution XPS spectra of I 3d (b) O 1s (c) and N 1s (d) for COF-Dha after I_2 (cyclohexane) adsorption.

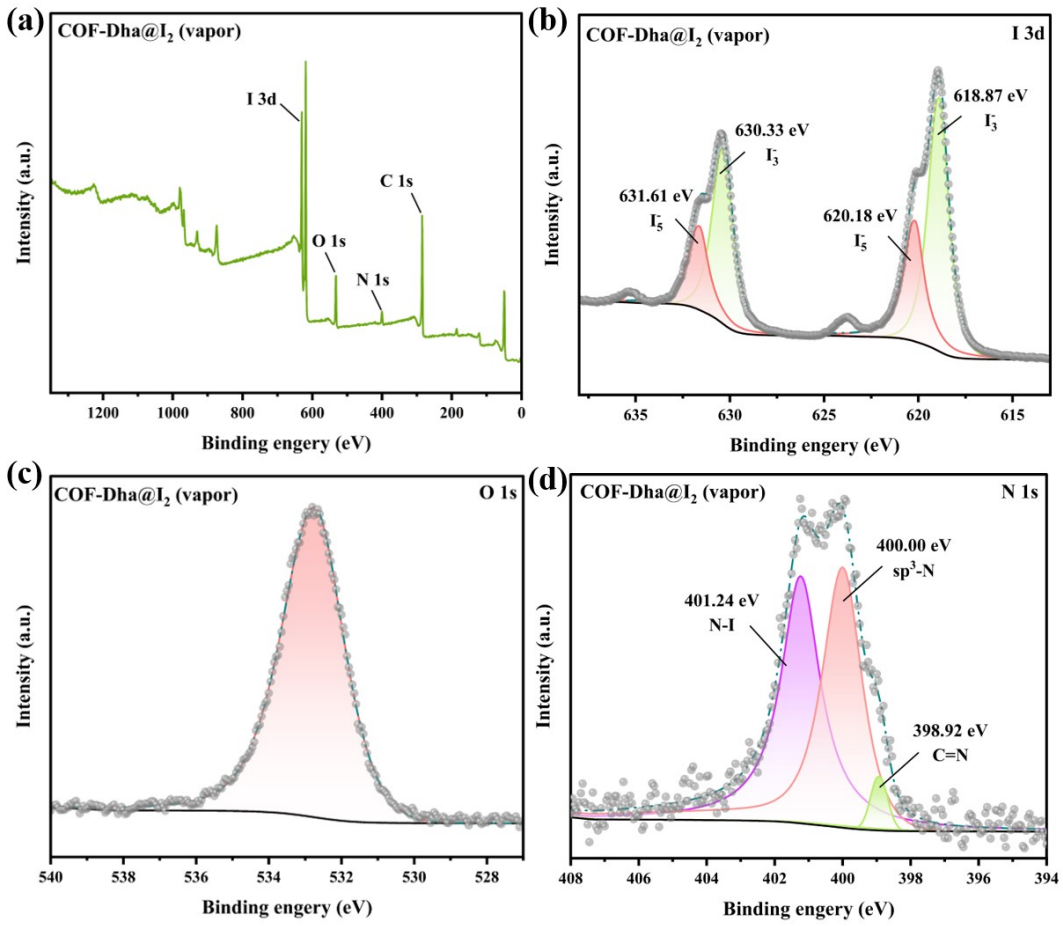

Figure S29. (a) Full survey XPS spectra of COF-Dha after I_2 (vapor) adsorption. High-resolution XPS spectra of I 3d (b) O 1s (c) and N 1s (d) for COF-Dha after I_2 (vapor) adsorption.

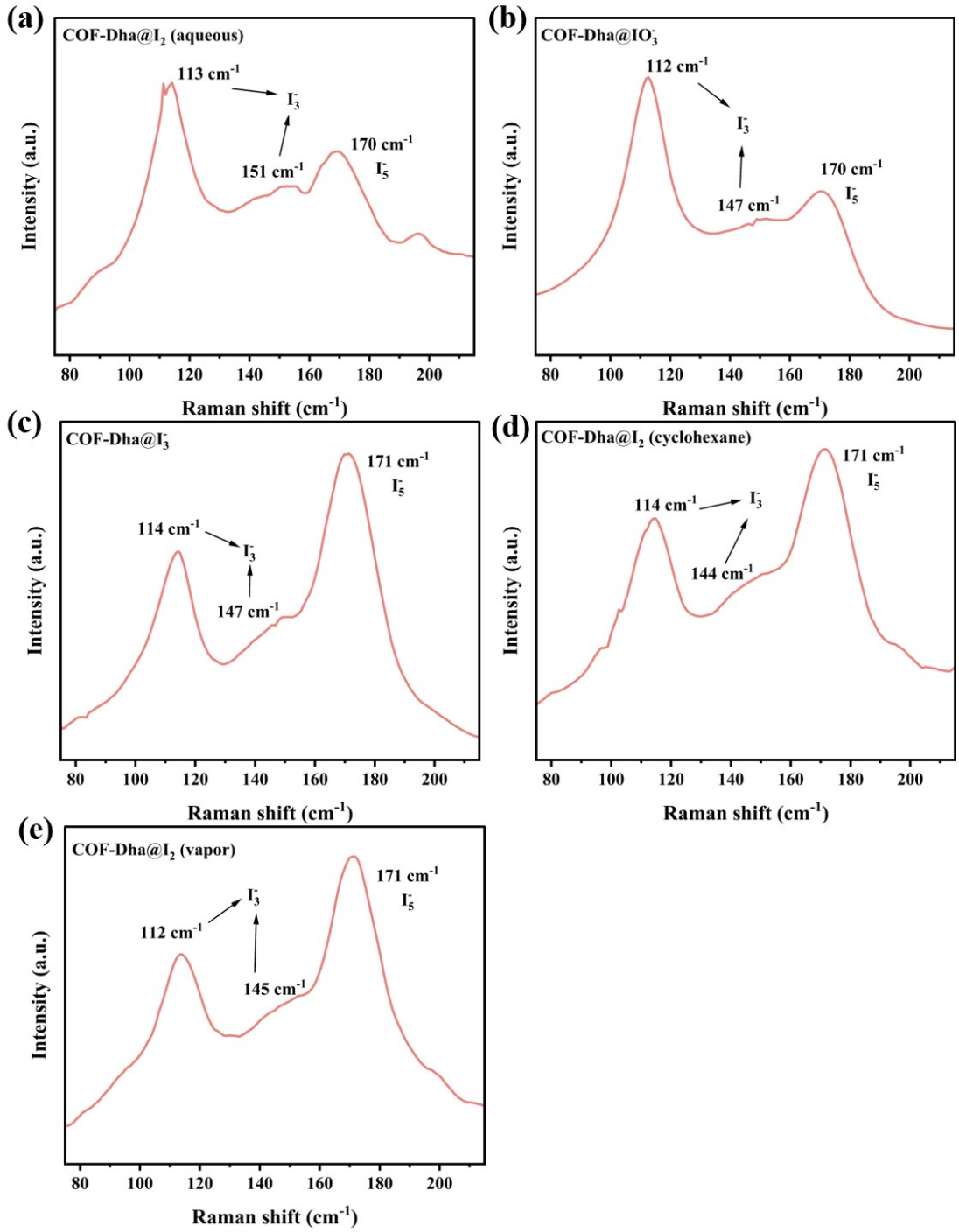

Figure S30. Raman spectra of COF-Dha@I_2 (aqueous) (a), COF-Dha@IO_3^- (b), COF-Dha@I_3^- (c), COF-Dha@I_2 (cyclohexane) (d) and COF-Dha@I_2 (vapor) (e).

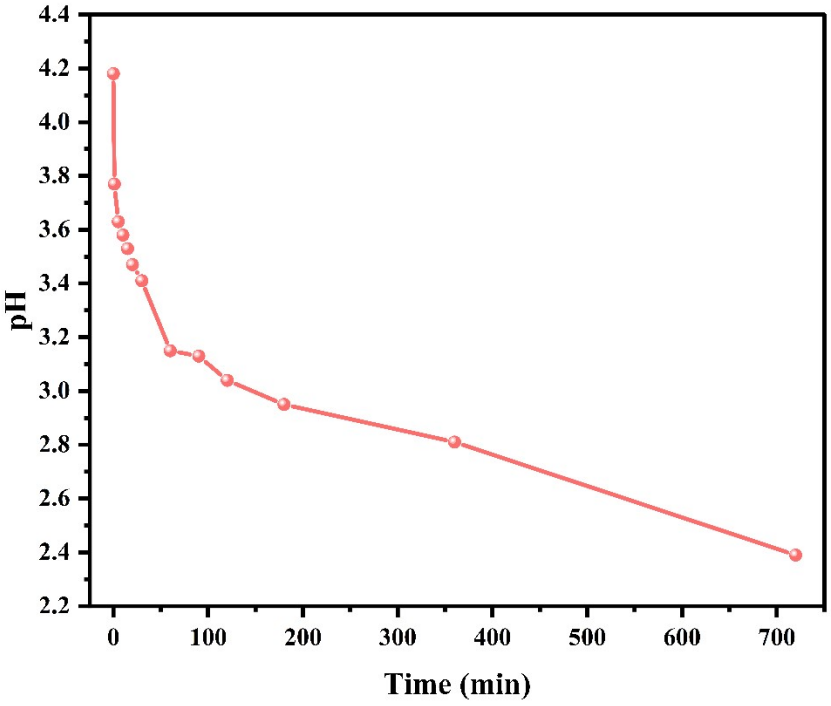

Figure S31. The change curve of pH in the adsorption process of saturated iodine water on COF-Dha.

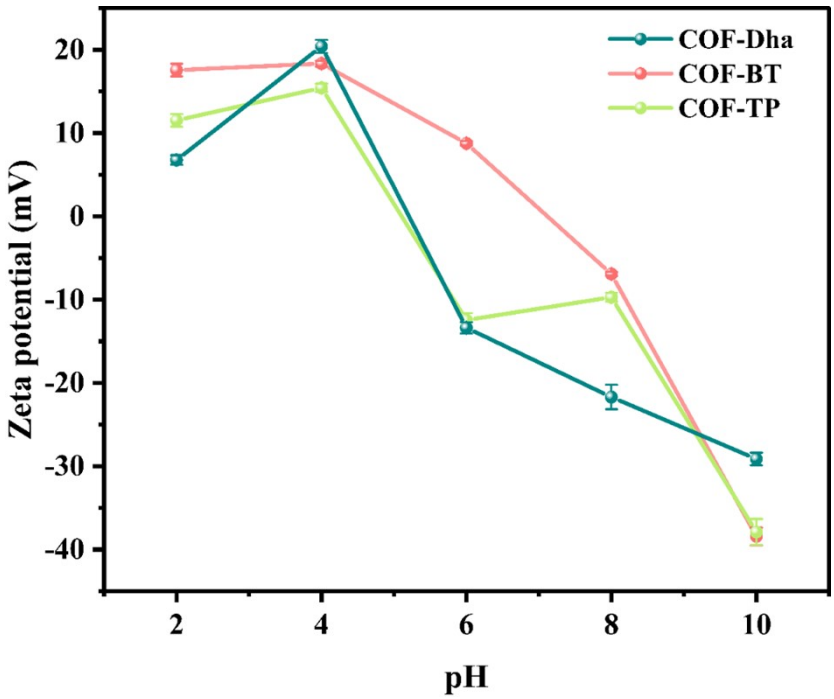

Figure S32. Zeta potential of COF-BT, COF-TP and COF-Dha under different pH.

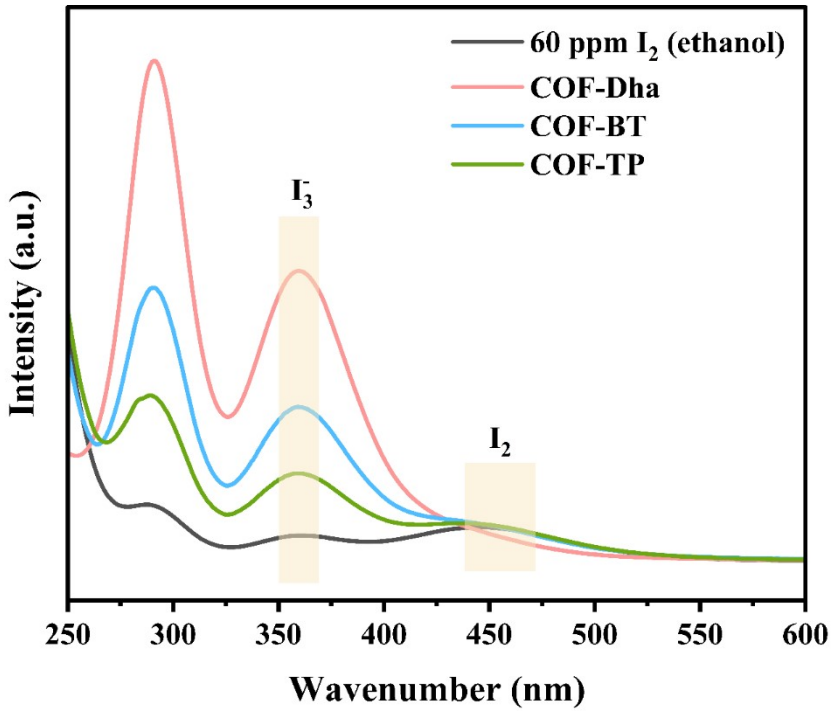

Figure S33. UV/vis spectra of COF-Dha in I_2-ethanol adsorption. (Initial 60 ppm, Solid-liquid ratio 0.1 g/L).

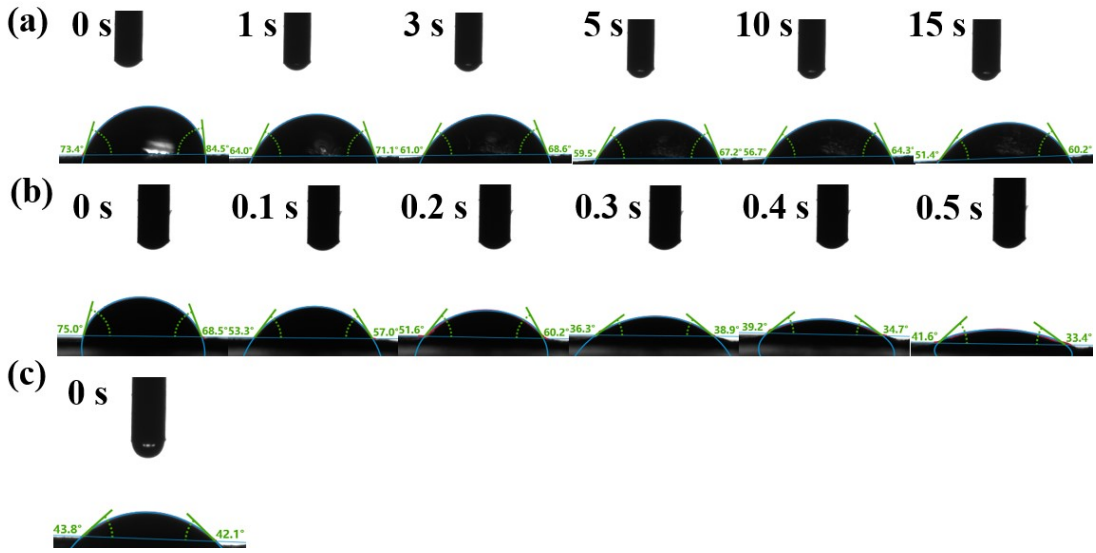

Figure S34. Contact angle of COF-Dha (a), COF-BT (b) and COF-TP (c).

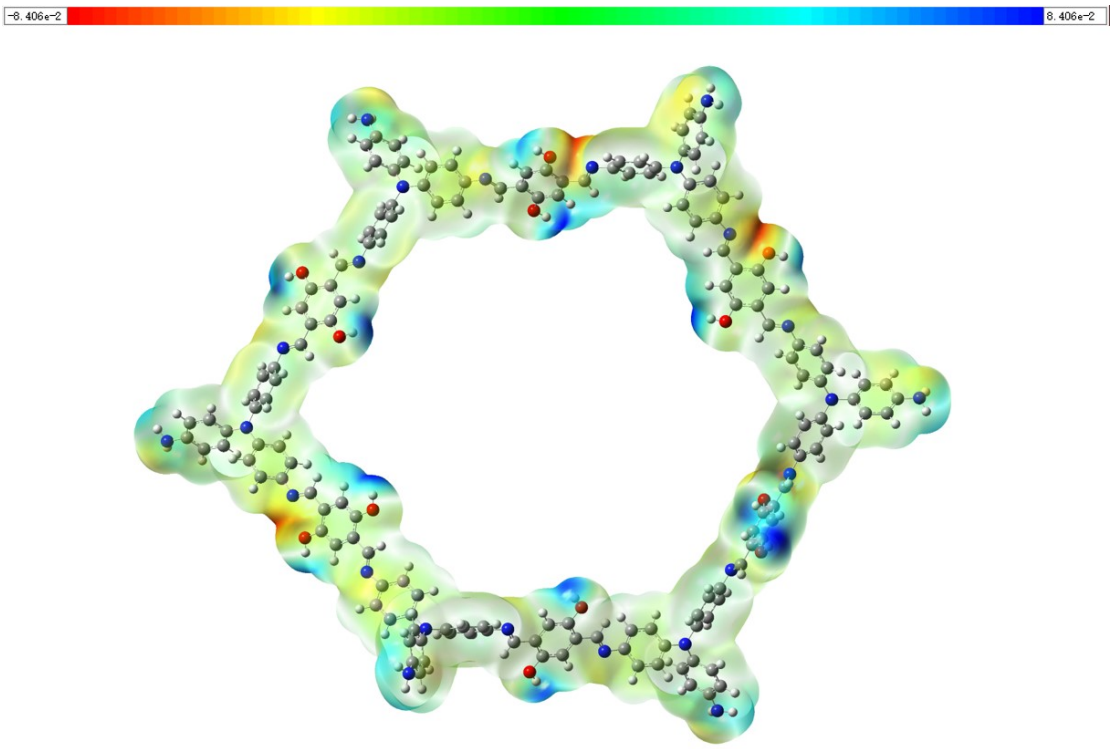

Figure S35. ESP analysis of COF-Dha.

Table S1. Comparison of I_2 (cyclohexane) adsorption performance across different adsorbents.

Number.	Adsorbents	I_2 (cyclohexane) capacity (g/g)	Refer
1	PHCP-3	0.062	[4]
2	PHCP-1	0.068	[4]
3	PHCP-4	0.116	[4]
4	TTPA-COF	0.129	[5]
5	PHCP-2	0.155	[4]
6	UiO-66	0.17	[6]
7	TAPT-COF	0.175	[7]
8	TAB-COF	0.2	[7]
9	Th-SINAP-7	0.352	[8]
10	COF-TP	0.37	This work
11	IMF-COP-Fe	0.393	[9]
12	Th-SINAP-8	0.473	[8]
13	BTD-PT	0.504	[10]
14	TTA-DMTP-COF	0.516	[11]
15	BTD-PB	0.537	[10]
16	TAC2	0.582	[12]
17	BTD-PA	0.665	[10]
18	MOF-74	0.68	[6]

19	TAC1	0.79	[12]
20	COF-BT	1.09	This work
21	TAC3	1.11	[12]
22	COF-Dha	1.26	This work
23	GOF-LS	1.32	[13]
24	TPATFB-COF	1.6	[14]

Table S2. Comparison of polyiodide adsorption performance on different adsorbents.

Number.	Adsorbents	polyiodide capacity (g/g)	Refer
1	IMF-COP-Fe	0.11	[15]
2	COF-V	0.44	[16]
3	OH-ExR4	0.62	[17]
4	HOF-TAM-BPY	0.67	[18]
5	COF-TP	0.86	This work
6	HOF-TAM-PNA	0.89	[18]
7	iPOP-6	1.02	[19]
8	3D MOF $\{[Mn_2(oxdz)_2(tpbn)(H_2O)_2]\cdot 2C_2H_5OH\}_n$	1.1	[20]
9	HOF-TAM-BDA	1.12	[18]
10	COF-BT	1.43	This work
11	COF-TMPT	1.55	[21]
12	C[4]P-DPP	1.58	[22]
13	iCON-4	1.63	[23]
14	ICOF-TG-DCA	2.21	[24]
15	pCAGE-2	2.24	[25]
16	COF-Dha	2.29	This work
17	C[4]P-BT	2.32	[22]
18	C[4]P-BP	2.37	[22]

19	COF-TCO	2.48	[26]
20	C[4]P-TTP	2.51	[22]
21	C[4]P-TPE	2.99	[22]
22	C[4]P-BTP	3.24	[22]
23	pCAGE-1	3.35	[25]
24	TPATFB-COF	3.9	[14]
25	IPcomp-7	5.16	[27]

Table S3. Kinetics parameters for I_2 vapor adsorption of COFs.

Sample	Pseudo-first-order		Pseudo-second-order	
COF-BT	$K_1(min^{-1})$	0.39	K_2 (g (g/ min)$^{-1}$)	0.08
	q_e (g·g^{-1})	4.60	q_e (g·g^{-1})	5.39
	R^2	0.9984	R^2	0.9993
COF-TP	$K_1(min^{-1})$	0.71	K_2 (g (g/ min)$^{-1}$)	0. 34
	q_e (g·g^{-1})	2.36	q_e (g·g^{-1})	2.56
	R^2	0.9974	R^2	0.9979
COF-Dha	$K_1(min^{-1})$	0.22	K_2 (g (g/ min)$^{-1}$)	0.04
	q_e (g·g^{-1})	4.73	q_e (g·g^{-1})	5.33
	R^2	0.9984	R^2	0.9998
COF-PDA	$K_1(min^{-1})$	0.35	K_2 (g (g/ min)$^{-1}$)	0.11
	q_e (g·g^{-1})	4.92	q_e (g·g^{-1})	5.36
	R^2	0.9996	R^2	0.9998

Table S4. Kinetics parameters for I_2-cyclohexane adsorption of COFs.

Sample	Pseudo-first-order		Pseudo-second-order	
COF-BT	$K_1(min^{-1})$	0.26	K_2 (mg (g/ min)$^{-1}$)	109
	q_e (mg·g^{-1})	94	q_e (mg·g^{-1})	96
	R^2	0.9995	R^2	0.9999
COF-TP	$K_1(min^{-1})$	0.02	K_2 (mg (g/ min)$^{-1}$)	3
	q_e (mg·g^{-1})	97	q_e (mg·g^{-1})	106
	R^2	0.9959	R^2	0.9974
COF-Dha	$K_1(min^{-1})$	0.14	K_2 (mg (g/ min)$^{-1}$)	32
	q_e (mg·g^{-1})	98	q_e (mg·g^{-1})	102
	R^2	0.9998	R^2	1.0000
COF-PDA	$K_1(min^{-1})$	0.21	K_2 (mg (g/ min)$^{-1}$)	96
	q_e (g·g^{-1})	94	q_e (g·g^{-1})	96
	R^2	0.9920	R^2	0.9984

Table S5. Parameters fitted for I_2-cyclohexane adsorption of COFs according to the Langmuir and Freundlich adsorption isotherms equations.

Models	Parm	Sample			
		COF-BT	COF-TP	COF-Dha	COF-PDA
Langmuir	Q_{max} ($g \cdot g^{-1}$)	1.09	0.37	1.26	1.10
	K_L (L/g)	0.02	1.44	0.02	0.01
	R^2	0.98	0.97	0.97	0.98
Freundlich	n	0.18	0.23	0.14	0.41
	K_F (($g \cdot g^{-1}$)*($L^{1/n} \cdot g^{-1/n}$))	0.29	0.13	0.36	0.09
	R^2	0.92	0.94	0.94	0.89

Table S6. Kinetics parameters for polyiodide adsorption of COFs.

Sample	Pseudo-first-order		Pseudo-second-order	
COF-BT	$K_1(min^{-1})$	0.40	K_2 (g (g/ min)$^{-1}$)	0.01
	q_e (g·g^{-1})	0.91	q_e (g·g^{-1})	0.95
	R^2	0.9854	R^2	0.9946
COF-TP	$K_1(min^{-1})$	0.15	K_2 (g (g/ min)$^{-1}$)	0.27
	q_e (g·g^{-1})	0.97	q_e (g·g^{-1})	0.99
	R^2	0.9820	R^2	0.9917
COF-Dha (50 ppm)	$K_1(min^{-1})$	0.21	K_2 (g (g/ min)$^{-1}$)	0.01
	q_e (g·g^{-1})	0.99	q_e (g·g^{-1})	1.05
	R^2	0.9987	R^2	0.9958
COF-Dha (100 ppm)	$K_1(min^{-1})$	0.04	K_2 (g (g/ min)$^{-1}$)	0.01
	q_e (g·g^{-1})	0.96	q_e (g·g^{-1})	0.99
	R^2	0.9976	R^2	0.9978

Table S7. Parameters fitted for polyiodide adsorption of COFs according to the Langmuir and Freundlich adsorption isotherms equations.

Models	Parm	Sample		
		COF-BT	COF-TP	COF-Dha
Langmuir	Q_{max} ($g \cdot g^{-1}$)	1.43	0.86	2.29
	K_L (L/g)	0.53	0.64	1.72
	R^2	0.93	0.99	0.93
Freundlich	n	0.14	0.12	1.87
	K_F (($g \cdot g^{-1}$)*($L^{1/n} \cdot g^{-1/n}$))	0.83	0.55	0.06
	R^2	0.86	0.95	0.86

Table S8. Kinetics parameters for IO_3^- adsorption of COF-Dha.

Pseudo-first-order		Pseudo-second-order	
$K_1(min^{-1})$	0.01	K_2 (g (g/ min)$^{-1}$)	0.03
q_e ($g \cdot g^{-1}$)	0.25	q_e ($g \cdot g^{-1}$)	0.29
R^2	0.9997	R^2	0.9999

Table S9. Parameters fitted for IO_3^- adsorption of COF-Dha according to the Langmuir and Freundlich adsorption isotherms equations.

Langmuir		Freundlich		
Q_{max} ($mg \cdot g^{-1}$)	467.18	n		295.00
K_L (L/g)	3.47	K_F	(($mg \cdot g^{-1}$)*($L^{1/n} \cdot g^{-1/n}$))	0.11
R^2	0.91	R^2		0.83

References

[1] A. F. M. EL-Mahdy, Y.-H. Hung, T. H. Mansoure, H.-H. Yu, Y.-S. Hsu, K. C. W. Wu, S.-W. Kuo, *J. Taiwan Inst. Chem. Eng.* **2019**, *103*, 199.

[2] Y. Huang, J. Liao, J. Li, C. Cheng, Y. Zhang, Y. Peng, *Chem. Commun.* **2024**, *60*, 1619.

[3] R. Chen, T. Hu, W. Zhang, C. He, Y. Li, *Microporous Mesoporous Mater.* **2021**, *312*, 110739.

[4] J. Ma, Z. Shi, T. Wang, X. Huang, Y. Zhao, J. Wang, J. Li, D. Wang, L. Sun, G. Dong, M. Zhao, *ACS Sustainable Chem. Eng.* **2024**, *12*, 12113.

[5] G. Shreeraj, A. Sah, S. Sarkar, A. Giri, A. Sahoo, A. Patra, *Langmuir* **2023**, *39*, 16069.

[6] T. Alghamdi, P. O. Aina, A. A. Rownaghi, F. Rezaei, *ACS Appl. Mater. Interfaces* **2023**, *15*, 33621.

[7] Y. Ran, Y. Wang, M. Yang, J. Li, Y. Zhang, Z. Li, *RSC Adv.* **2024**, *14*, 32451.

[8] Z.-J. Li, Z. Yue, Y. Ju, X. Wu, Y. Ren, S. Wang, Y. Li, Z.-H. Zhang, X. Guo, J. Lin, J.-Q. Wang, *Inorg. Chem.* **2020**, *59*, 4435.

[9] Y. Shen, J. Zhang, Y. Wang, X. Li, *New J. Chem.* **2025**, *49*, 3536.

[10] Y. Ji, J. Huang, C. Liu, C. Ni, H. Yan, Y. David, Y. Qin, *ACS Appl. Polym. Mater.* **2024**, *6*, 7478.

[11] W.-Z. She, Q.-L. Wen, H.-C. Zhang, J.-Z. Liu, R. S. Li, J. Ling, Q. Cao, *ACS Appl. Nano Mater.* **2023**, *6*, 18177.

[12] S. Shetty, N. Baig, B. Pallavi, R. Bargakshatriya, S. K. Pramanik, B. Alameddine, *Mater. Adv.* **2025**.

[13] N. Naseri, R. Azadi, H. Motamedi, T. Sedaghat, *ACS Appl. Nano Mater.* **2024**, *7*, 16475.

[14] S. Kumar, N. Desai, B. Z. Dholakiya, S. N. Yethadka, R. Jangir, *Langmuir* **2025**, *41*, 26166.

[15] Y. Shen, J. Zhang, Y. Wang, X. Li, *New J. Chem.* **2025**, *49*, 3536.

[16] X. Tian, G. Zhou, J. Xi, R. Sun, X. Zhang, G. Wang, L. Mei, C. Hou, L. Jiang, J. Qiu, *Sep. Purif. Technol.* **2023**, *310*, 123160.

[17] D. Li, G. Wu, Y.-K. Zhu, Y.-W. Yang, *Angew. Chem. Int. Ed.* **2024**, *63*, e202411261.

[18] Y. Wang, Y. Jin, W. Xian, X. Zuo, S. Wang, Q. Sun, *J. Mater. Chem. A* **2022**, *10*, 18730.

[19] A. Hassan, R. K. Pandey, A. Chakraborty, S. A. Wahed, T. R. Rao, N. Das, *Soft Matter* **2024**, *20*, 7832.

[20] A. Gogia, P. Das, S. K. Mandal, *ACS Appl. Mater. Interfaces* **2020**, *12*, 46107.

[21] Y. Tang, Z. He, W. Xue, H. Huang, G. Zhang, *Chem. Eng. J* **2023**, *470*, 144211.

[22] L. Xie, Z. Zheng, Q. Lin, H. Zhou, X. Ji, J. L. Sessler, H. Wang, *Angew. Chem. Int. Ed.* **2022**, *61*, e202113724.

[23] Prince, A. Hassan, S. Chandra, A. Alam, N. Das, *RSC Sustainability* **2023**, *1*, 511.

[24] X. Guan, Z. Shen, L. Chen, C. Zhang, C. Sun, Y. Du, B. Hu, C. Gao, *ACS Appl. Nano Mater.* **2024**, *7*, 27318.

[25] F. Begar, M. Erdogmus, Y. Gecalp, U. C. Canakci, O. Buyukcakir, *ACS Appl. Polym. Mater.* **2024**, *6*, 5358.

[26] S. Saurabh, S. Mollick, Y. D. More, A. Banerjee, S. Fajal, N. Kumar, M. M. Shirolkar, S. B. Ogale, S. K. Ghosh, *ACS Materials Lett.* **2023**, *5*, 2422.

[27] S. Fajal, W. Mandal, A. Torris, D. Majumder, S. Let, A. Sen, F. Kanheerampockil, M. M. Shirolkar, S. K. Ghosh, *Nat. Commun.* **2024**, *15*, 1278.